RADC-TR-65-247
Final Report

STRUCTURAL STUDY OF AN/FPS-24 PEDESTAL

H. D. Barnhurt
J. M. McGrew
E. Lange
(G.E.)

TECHNICAL REPORT NO. RADC-TR-65-247
September 1965

Development Engineering Branch
Rome Air Development Center
Research and Technology Division
Air Force Systems Command
Griffiss Air Force Base, New York

STRUCTURAL STUDY OF AN/FPS-24 PEDESTAL

H. D. Barnhart
J. M. McGrew
E. Lange
(G.E.)

AFLC, GAFB, N.Y., 13 Oct 65-115

FOREWORD

This report was prepared by the Heavy Military Electronics Department of General Electric Co., Syracuse, N.Y. under Contract AF30(602)-3567. The work was performed under system 416L. The RADC Project Engineer was Mr. John J. Gugino.

The Heavy Military Electronics Department wishes to acknowledge the assistance, cooperation, encouragement, and contributions to the program by the following personnel:

J. Scheiderich	Rome Air Development Center
J. Gugino	Rome Air Development Center
O.G. Kristensen	Advanced Technology Lab (GE-Schenectady)
J.M. McGrew	Advanced Technology Lab (GE-Schenectady)
H.D. Barnhart	Electronics Lab, GE-Syracuse
E.V. Pearse	Electronics Lab, GE-Syracuse
G.F. Trojanowski	Materials and Processes Lab, GE-Syracuse
F. Hirth	FAA Chief, Oakdale, Pa.
E. Ellis	FAA Chief, Malmstrom, Montana

This technical report has been reviewed and is approved.

Approved: John J. Gugino

JOHN J. GUGINO
Structural Engineering Group
Mechanical Engineering Section

Approved: William P. Bethke

WILLIAM P. BETHKE
Chief, Engineering Division

FOR THE COMMANDER: Irving Gabelman

IRVING GABELMAN
Chief, Advanced Studies Group

ABSTRACT

Purpose

The main purpose of this program was to determine the actual static load distribution of the AN/FPS-24 main azimuth bearing and determine the effect of this distribution on the theoretical life of the bearing.

In addition to the above, the program required the design, fabrication, and feasibility testing of a "calipered" ball device which could possibly be used to obtain actual dynamic (operating) load data.

Course of Action

The methods to be utilized for obtaining the actual static load data were established and the required materials obtained. These methods were respectively, a strain gaged load cell and the measurement of contact ellipse. Concurrent with the program for obtaining static load data, a "calipered" ball device was designed and fabricated.

Static load data was obtained by both methods selected and feasibility tests conducted on the "calipered" ball device.

The static load data was analyzed and computer computations made for bearing life. Comparisons were made between theoretical life based on calculated loads and theoretical life based on actual measured loads.

Results

Static load data obtained by both methods selected was consistent and in close agreement with theoretical calculated data.

Computations of bearing life show no significant difference when computed on the basis of calculated loads or measured loads.

Feasibility tests conducted on the "calipered" ball device show the device to be capable of obtaining dynamic data. Initial data obtained as part of the feasibility tests appear to indicate that dynamic loads may be significantly different than calculated dynamic loads.

Conclusions

Conclusions reached are as follows:

1. Since the calculated and measured loads are in close agreement there can be no significant difference in the calculated bearing life.
2. Temperature changes do not appear to have a significant effect on load.
3. The "calipered" ball device is capable of obtaining dynamic data.
4. Dynamics of operation appear to be highly significant and the associated loads must be known in order to accurately calculate bearing life.

TABLE OF CONTENTS

CHAPTER 1

DETERMINATION OF ROLLING ELEMENT LOAD DISTRIBUTION BY STATIC METHODS AND THE FEASIBILITY OF DYNAMIC LOAD DETERMINATION BY CALIPERED METHOD

TABLE OF CONTENTS (cont)

CHAPTER 2

AN EVALUATION OF THE MEASURED LOAD DISTRIBUTION FOR THE AN/FPS-24 ANTENNA BEARING

LIST OF ILLUSTRATIONS

LIST OF TABLES

NOMENCLATURE

a	=	semimajor axis of contact ellipse, in.
A	=	fatigue constant for bearing
b	=	semiminor axis of contact ellipse, in.
d	=	Ball diameter, in.
e	=	coefficient in life formula
E	=	pitch diameter, in.
f	=	ratio of transverse radius of ball race to ball diameter
F	=	force
g	=	function used in calculation of ball load
B^L	=	fatigue life for ball bearing, hr.
n	=	number of rolling elements
N	=	speed of rotating race, rpm
P	=	rolling element load, lb.
Q_{cq}	=	capacity of ball race contact for 90 per cent probability of survival to 10^6 revolutions of inner race
x, y, z	=	Bearing Coordinate system
θ	=	Ball position from boom, degrees

Subscripts

- i = inner race
- o = outer race
- q = q^{th} rolling element

INTRODUCTION

Historically, the life performance of large diameter rolling element bearings has been significantly less than the theoretically calculated life based on "state of the art" methods.

Over the past several years numerous studies and investigations have been conducted and improvements made in the areas of lubrication, metallurgy, inspection techniques, quality control, lubricant filtration, truing of bearing seats, and other innovations such as rolling element load slots and nital etching of rolling elements.

While all these areas have contributed to improved operation they have not resulted in the degree of performance desired.

Recognizing that actual rolling element loads could result in a more accurate determination of bearing life the Air Force implemented this program to obtain actual data.

This program was undertaken by the Heavy Military Electronics Department with assistance from the Electronics Laboratory and Advanced Technology Laboratory all of the General Electric Company, in an effort to provide the Air Force with the data for predicting bearing life more accurately.

CHAPTER 1

DETERMINATION OF ROLLING ELEMENT LOAD DISTRIBUTION BY STATIC METHODS AND THE FEASIBILITY OF DYNAMIC LOAD DETERMINATION BY CALIPERED METHOD

SECTION A. STATIC LOAD CELL MEASUREMENT DISCUSSION

1. Static Measurement Concept. To obtain a better understanding of life predicting data for the FPS-24 azimuth bearing, a static ball distribution load measuring method was developed. This measurement technique uses a section of a normal ball bearing ball functioning as a static load cell. This ball bearing section load cell is then adapted to placement within the bearing without significant modification from normal operation. The slight modification consists of either removing one ball through the load slot or the possibility of respacing balls to create an empty ball slot through the use of the flame gap for a movement area. In general, the empty ball slot is advanced to each location where it is possible to remove the separator and static load measurements obtained for that position.

A second method to support the load cell technique was also used at the Oakdale Site. This method consisted of a special adaptation of brush plating a few microinches of soft, dull-finish tin on the inner and outer races in the ball path area. The antenna was then advanced to a position bringing the ball in contact with the tin plate and then backed off to its original position. Load information then was determined by a measurement of the length of the major axis of the ball contact load ellipse.

2. Load Cell Design. To obtain the best possible load-matching characteristics for the load cell, it was decided to obtain the load cell from a section directly through the middle of a bearing ball of diameter equal to that used at Oakdale. The size of this load cell was dictated by strength, sensitivity, and stiffness. Strain gages were affixed to the load cell in such a way that positioning of the cell within the races was not critical.

Two additional gages were fastened to the load cell to supply information as to load angle of contact of the load applied to the load cell. The reading from these two strain gages having a sensitivity of approximately one-quarter of a degree, indicated when the load cell was directly in line with the load angle.

3. Use of Load Cell. In order to use the static load cell, one ball was removed from the bearing and the keeper was left off of that particular separator. This permitted rotation of the antenna to progress the empty ball slot to the desired location. At the desired location the separator was removed, the load cell inserted in the empty ball slot and jockeyed into place as nearly in line as possible. With the load cell held in this position, the antenna was rotated slightly to move the load cell in direct line with the axis of the maximum load. With the load cell in this position, two strain gages indicating angle of load were checked to determine if the correct load angle had been set. In the event that the load angle was incorrect, the antenna was moved in the reverse direction and the cell removed. The load angle was adjusted in the correct direction. Then the cell was re-inserted and the above procedure repeated until the correct angle was obtained. (See Figure 1). At this point, the strain gage amplifier was attached to the load cell to determine actual load applied to the load cell itself.

Using this procedure, loads at various azimuth positions were obtained for four different conditions of boom position and boom load. This data is shown in Tabulations 1, 2, 3, and 4 and plotted on Curves 1, 2, 3, and 4.

4. Load Ellipse Method. With the antenna correctly placed (slightly CCW from the test location) the bearing race ball paths were brush plated using a dull-finish tin coating a few microinches thick. This tin plating was applied by a brush-plating technique using cotton swabs and observing with two mirrors. Following this plating, the antenna was advanced to the zero boom position and returned to its position slightly CCW. This movement advanced each of the balls into the area previously tin plated, with the resultant ball path brightening the dull-tin finish the exact width of the area of contact of the ball with the

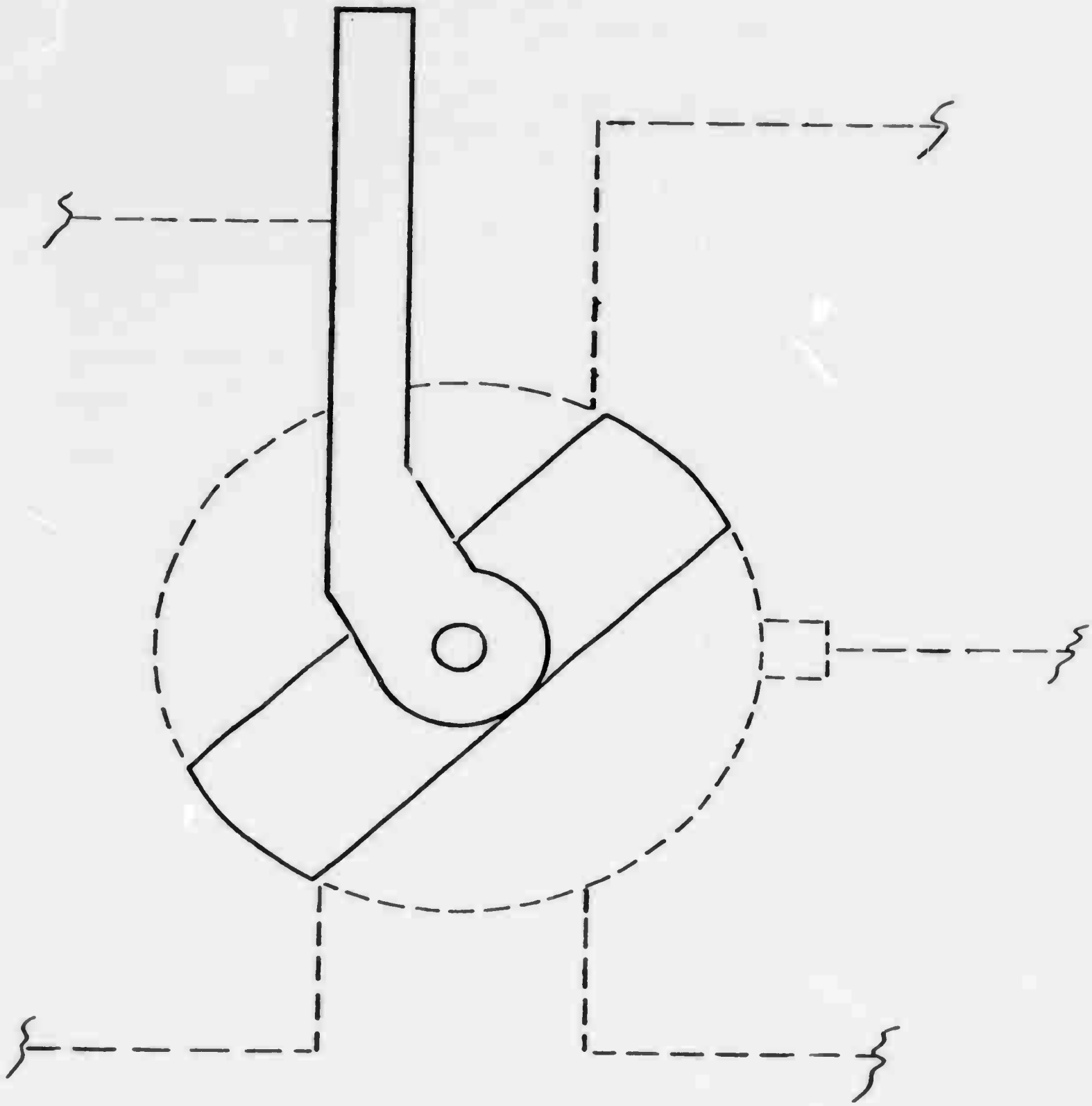

Figure 1. Static Load Cell in Position

Boom Position 0 (± 5°)

Condition No Load

Remarks

Date 1-13-65

Position Ball No.	Wind Velocity	Wind Direction	Load Angle	Load Major lbs.	Load Minor lbs.	Contact Ellipse Major	Contact Ellipse Minor
2	20	SW	35	4220	0		
2	14	SW	34	4150	0		
4	12	SW	35	4220	0		
5	9	SW	35	3520	0		
8	5	SW	34.25	4450	0		
10	13	SW	35	4980	0		
13	10	WSW	34	4850	0		
15	9	WSW	35	4190	0		
18	9	WSW	34.25	3920	0		
20	12	WSW	35	4150	0		
24	11	SW	34	3620	0		
26	11	SW	34	4100	0		
30	22	N	34	3820	0		
33	22	SW	36	3920	0		
39	12	WSW	35	3300	0		
44	10	WSW	35	3420	0		
47	10	SW	35	4100	0		
50	10	SW	33.5	4980	0		
50	15	SW	33.75	5010	0		
52	11	SW	34.50	4840	Trace		
54	14	SW	33.50	4920	0		
58	11	WSW	35	3920	0		
60	5	WSW	34.5	3880	0		
63	10	WSW	35	3720	0		
67	13	SW	35	3720	0		
69	15	SW	34.5	4220	0		
71	25	NW	36.0	4190	0		
71	15	NW	36.0	4100	0		
76	18	W	35.5	4400	0		
78	14	SW	34.5	4450	0		
82	13	WSW	35	4400	0		
64-65	Flame Gap						
74-75	Load Slot			Tabulation No. 1			

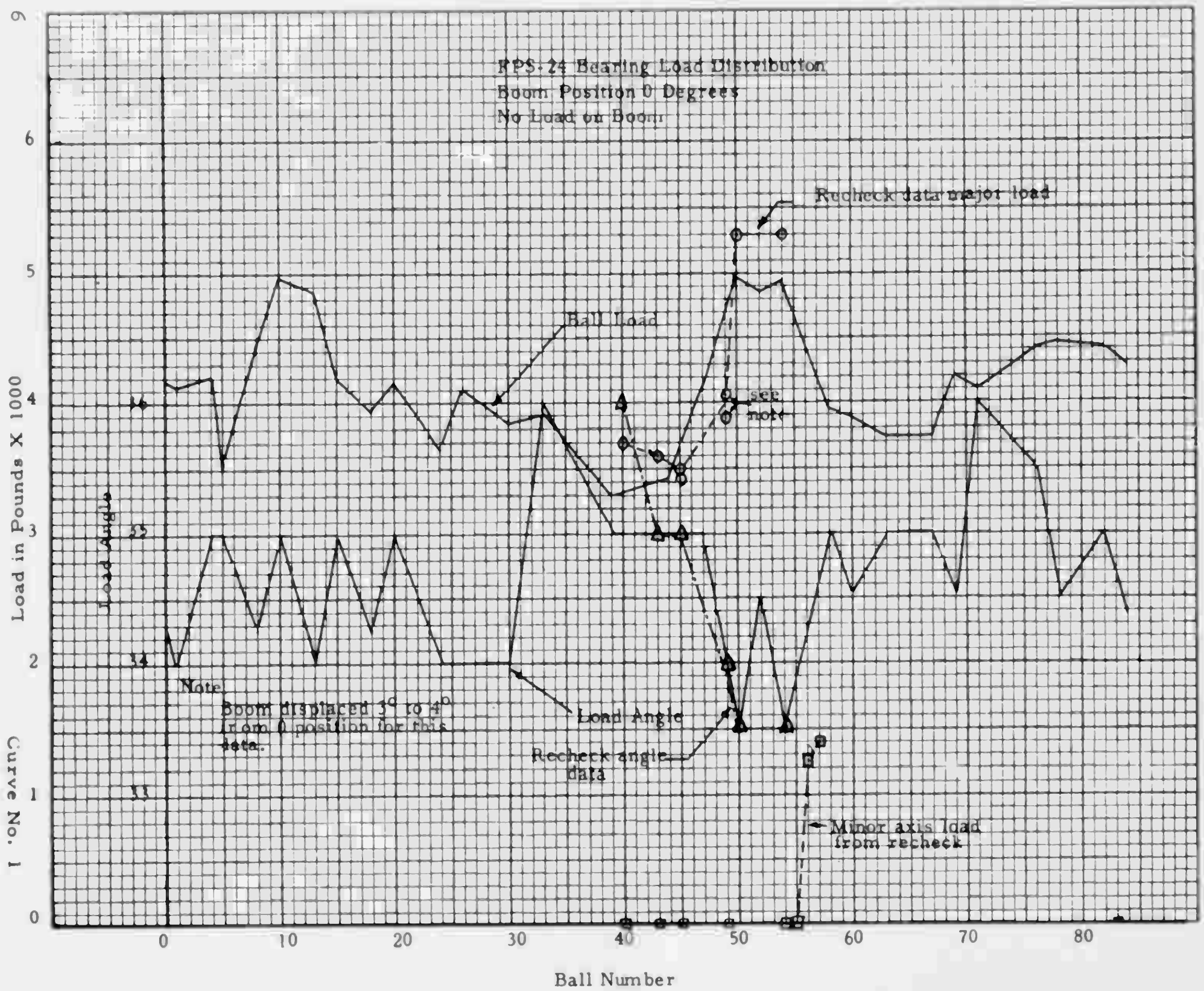
RPS-24 Bearing Load Distribution
Boom Position 0 Degrees
No Load on Boom
Recheck data major load
Ball Load
see note
Load Angle
Note
Boom displaced 3° to 4° from 0 position for this data.
Load Angle
Recheck angle data
Minor axis load from recheck
Load in Pounds X 1000
Curve No. 1
Ball Number
0
1
2
3
4
5
6
9
0
10
20
30
40
50
60
70
80
33
34
35

Boom Position 0 (± 5°)

Condition 3000 # Load

Remarks

Date 1-17-65

Position Ball No.	Wind Velocity	Wind Direction	Load Angle	Load Major lbs.	Load Minor lbs.	Contact Ellipse Major	Contact Ellipse Minor
1	11	SW	35	4200	0		
4	7	SW	34.75	5060	0		
6	15	SW	33.5	5450	0		
6	10	SW	33.5	5400	0		
10	15	SW	33.25	5530	0		
15	5	SW	34	4710	0		
18	14	SW	34	4200	0		
20	14	WSW	34	3780	0		
22	19	SW	33.5	3590	0		
26	10	SW	33.5	3730	0		
31	9	SW	33.5	4290	Trace		
38	6	SW	34	3630	0		
43	5	SW	33.5	3790	SL. Trace		
48	5	SW	33.5	5005	Trace		
54	4	SW	34	3680	0		
57	5	SW	34	3630	0		
69	20	SW	34.5	3680	0		
72	10	SW	34	4890	0		
75	9	SW	34	4530	0		
79	16	SW	34.5	3490	0		
83	15	SW	34.5	4405	0		
64-65	Flame Gap						
74-75	Load Slot						

Tabulation No. 2

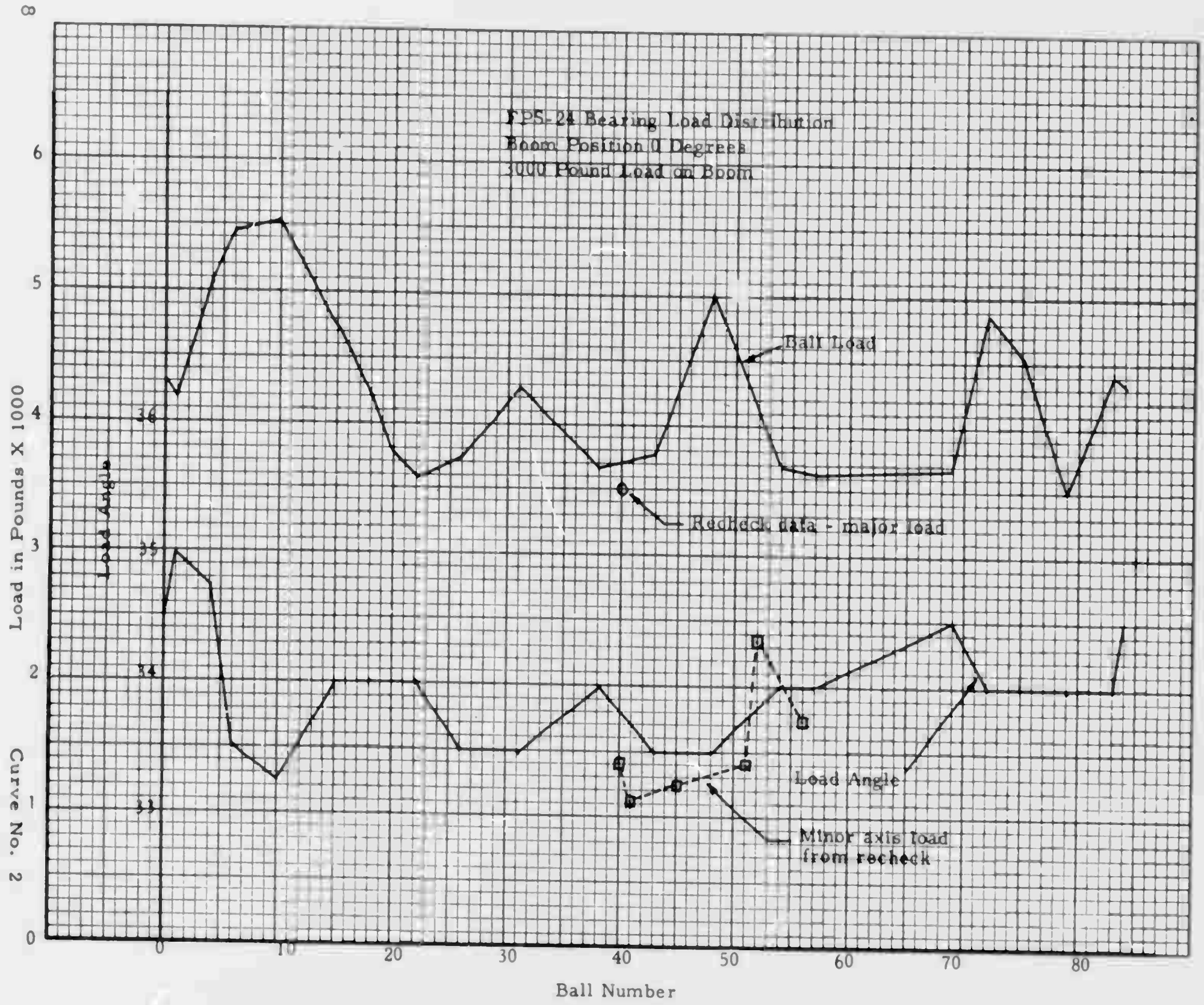
FPS-24 Bearing Load Distribution
Boom Position 0 Degrees
3000 Pound Load on Boom
Ball Load
Recheck data - major load
Load Angle
Minor axis load from recheck
Load in Pounds X 1000
Curve No. 2
Ball Number
0
1
2
3
4
5
6
10
20
30
40
50
60
70
80
36
35
34
33

Boom Position 315 (± 5 o)

Condition No Load

Date 1-13-65

Remarks

Position Ball No.	Wind Velocity	Wind Direction	Load Angle	Load Major lbs.	Load Minor lbs.	Contact Ellipse Major	Contact Ellipse Minor
1	13	SW	34	4540	0		
3	12	WSW	34.75	4890	0		
6	6	WSW	33	4060	0		
8	13	WSW	35	4100	0		
12	8	WSW	35	4200	0		
17	9	WSW	35	3420	0		
21	15	N	34	4680	0		
24	10	N	34	4760	0		
27	20	SW	33.5	4710	0		
31	13	SSW	33.5	4220	0		
33	15	SSW	33.5	4800	0		
37	12	SW	33.5	3780	0		
42	15	SW	34	3820	0		
43	7	SW	34	4630	0		
46	12	SW	35	4800	Trace		
50	11	WSW	35	3480	0		
52	11	WSW	35	3570	0		
56	10	WSW	34.5	3520	0		
60	13	SW	34.5	4010	0		
62	12	SW	34	3820	0		
66	15	NW	34	4400	0		
70	15	W	36.5	4540	0		
70	10	SSW	36.5	4460	0		
76	14	SW	35	4890	0		
80	15	SW	35	4405	0		
81	10	SW	34	5070	0		
52-53	Flame Gap						
74-75	Load Slot						

Tabulation No. 3

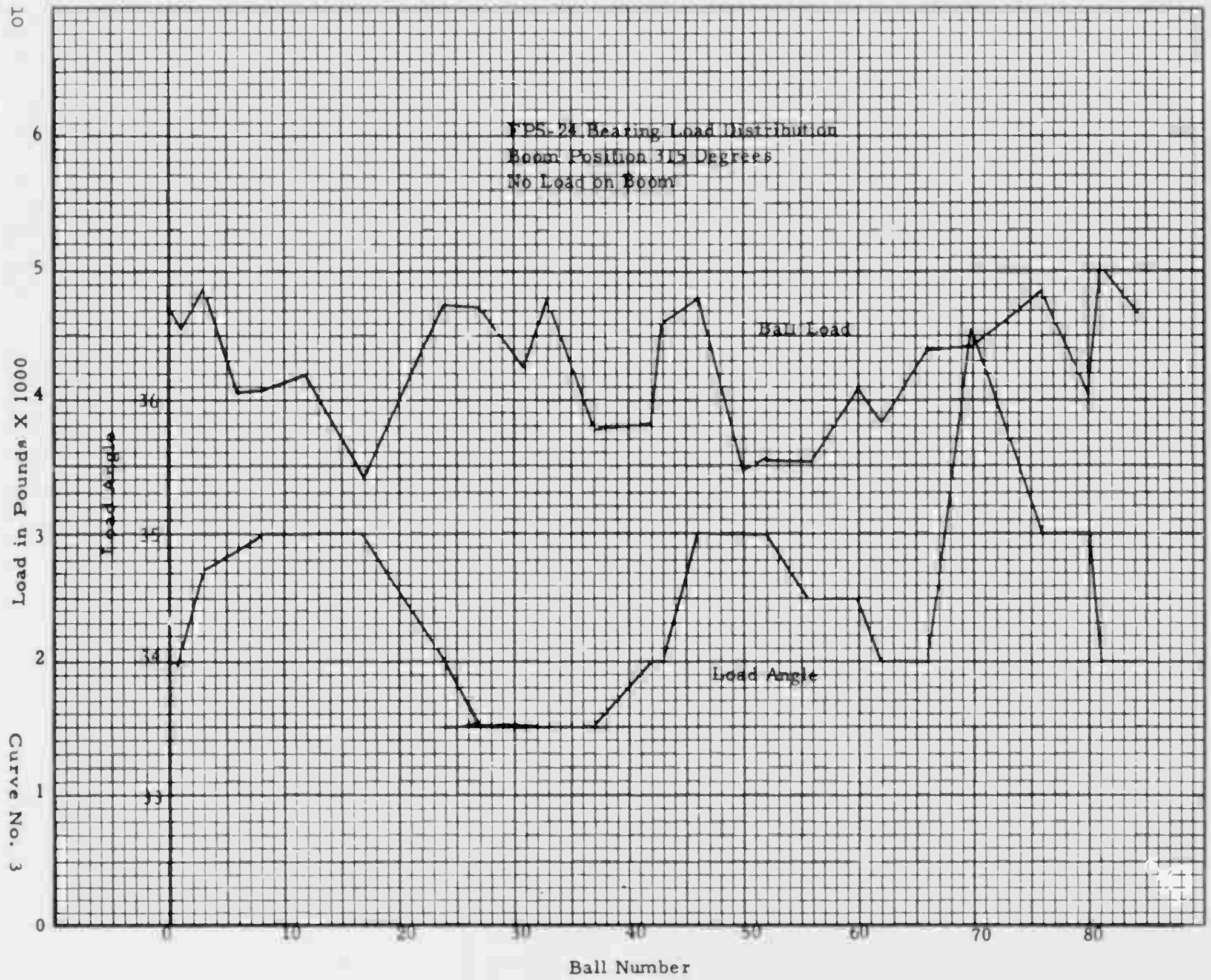
FPS-24 Bearing Load Distribution
Boom Position 315 Degrees
No Load on Boom
Ball Load
Load Angle
Load in Pounds X 1000
Load Angle
Curve No. 3
Ball Number
0
1
2
3
4
5
6
10
36
35
34
33
0
10
20
30
40
50
60
70
80

Boom Position 315 (± 5 °) Date 1-17-65

Condition 3000# Load

Remarks

Position Ball No.	Wind Velocity	Wind Direction	Load Angle	Load Major lbs.	Load Minor lbs.	Contact Ellipse Major	Contact Ellipse Minor
3	6	SW	34.5	4890	0		
8	6	SW	33.5	4150	0		
15	17	WSW	34	3200	0		
29	8	SW	33.5	4450	0		
36	7	SW	34.5	4700	0		
41	5	SW	34	4380	Trace		
45	4	SW	34	4150	Trace		
50	4	SW	34	3620	0		
56	5	SW	33.5	4190	0		
59	19	SW	33.5	4400	0		
62	17	SW	34.5	3680	0		
66	11	SW	33.75	3910	0		
68	12	SW	34	4540	0		
72	14	SW	34.5	4890	0		
78	17	SW	34.25	4370	0		
83	15	SW	34	4540	0		
52-53	Flame Gap						
74-75	Load Slot						

Tabulation No. 4

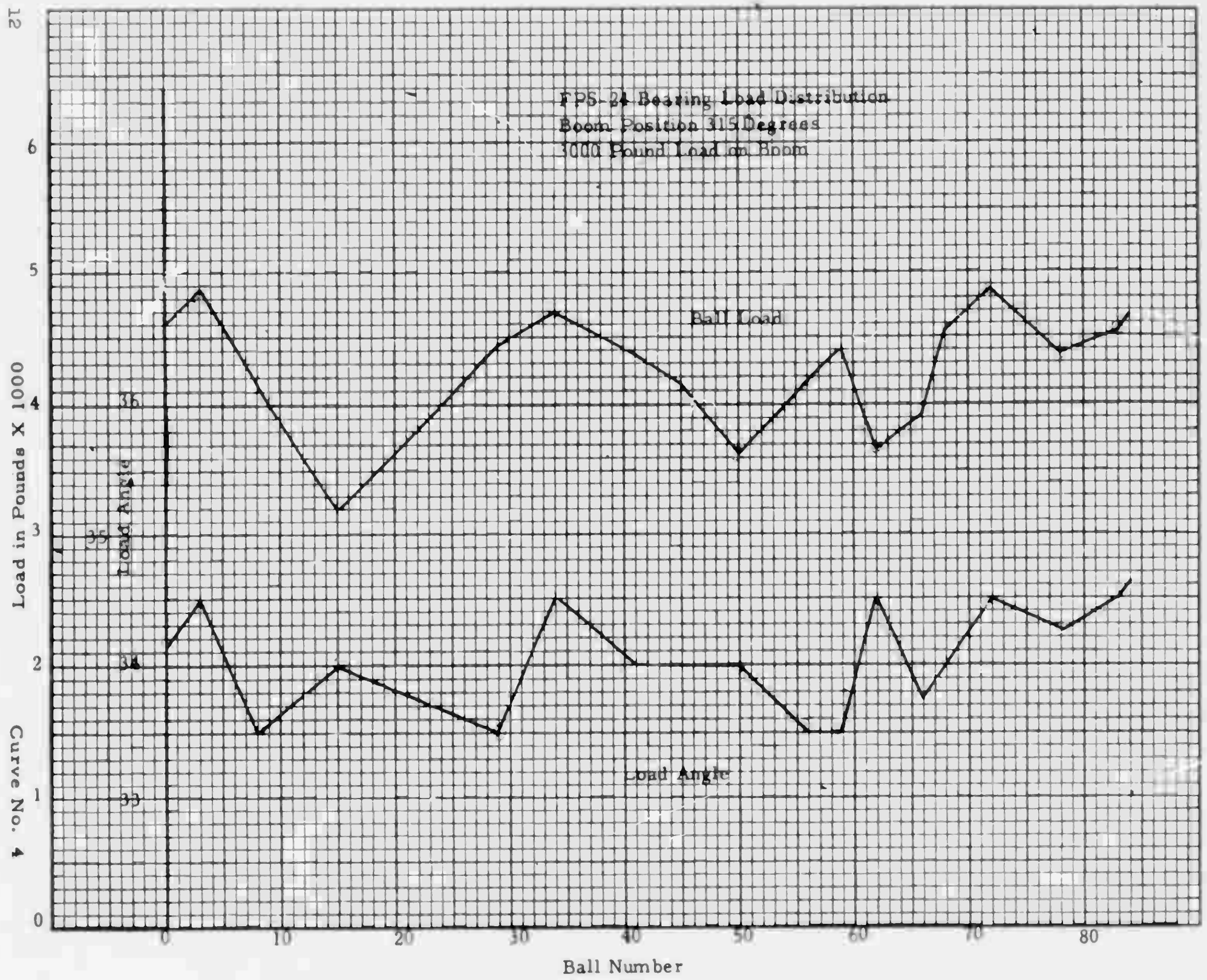
FPS-24 Bearing Load Distribution
Boom Position 315 Degrees
3000 Pound Load on Boom
Ball Load
Load Angle
Load in Pounds X 1000
Curve No. 4
Load Angle
Ball Number
0
1
2
3
4
5
6
12
33
34
35
36
0
10
20
30
40
50
60
70
80

outer or inner race. Following the reading of the major axis at this contact area, 3000 pounds was added to the boom and the next test taken. This time the movement of the balls into the tin-plated area was approximately one-quarter of an inch beyond the first test. The antenna was then moved back CCW and this data recorded as before. This data is shown in Tabulations 5 and 6 and is plotted on Curves 5 and 6.

5. Difficulty in Obtaining Loads. Several difficulties were encountered in advancing the antenna to the correct position with one or all of the keepers removed as required during the tests. The first problem was the bunching of the separators, causing them to push up whenever the antenna was rotated with the keepers removed. To resolve this it was necessary to cut two-by-eight lumber to go between the gussets and slide along on top of the separators. Following the load ellipse test, all but one of the keepers were then reassembled. Even under this condition the one separator had a strong tendency to ride up.

There were two types of separator tightness problems; the first was a tendency for separators in a large arc to bunch up and become very tightly wedged together. In the event that the ball slot was contained in this grouping, it was impossible for the separator to be removed to make load cell measurements. The only solution was to continually move the antenna back and forth until this condition was worked loose; at times this took several hours.

The second condition of tightening resulted when two adjacent balls advanced at different speeds. This held the separator in place and prevented its being removed for measurements. This was also the condition which bothered the tests most of all, since it had a tendency to squirt the separator out of the bearing. Therefore, any movement of the antenna required 100 percent observation to stop this condition the instant that the separators started to ride up. The separator could be pushed back down by applying force on top of the separator and moving the antenna back and forth.

Boom Position 0

Condition No Load

Remarks

Date 1-12-65

Position	Wind Velocity	Wind Direction	Load Angle	Load Major	Load Minor	Contact Ellipse Major	Contact Ellipse Minor
9	13	N				3700	
15	13	N				5150	
17	13	N				3700	0
61	13	N				3700	
65	13	N				2300	
69	13	N				3000	0
74	13	N				3000	
95	13	N				4400	
98	13	N				5450	
104	13	N				5150	Trace
108	13	N				3700	
128.5	13	N				4400	
134	13	N				5150	
138	13	N				3000	0
142.5	13	N				3600	
181	13	N				4400	
186	13	N				4400	Sl. Trace
189	13	N				3700	
194	13	N				4050	
215	13	N				4050	
219	13	N				4400	
224	13	N				4400	0
228	13	N				4050	
268	13	N				4400	
272	13	N				4400	0
280	13	N				4400	
302	13	N				3700	
337	13	N				5150	
339	13	N				4400	
344	13	N				5150	0
348	13	N				5150	
52-53	Flame Gap						
74-75	Load Slot						

Tabulation No. 5

0° - No Load

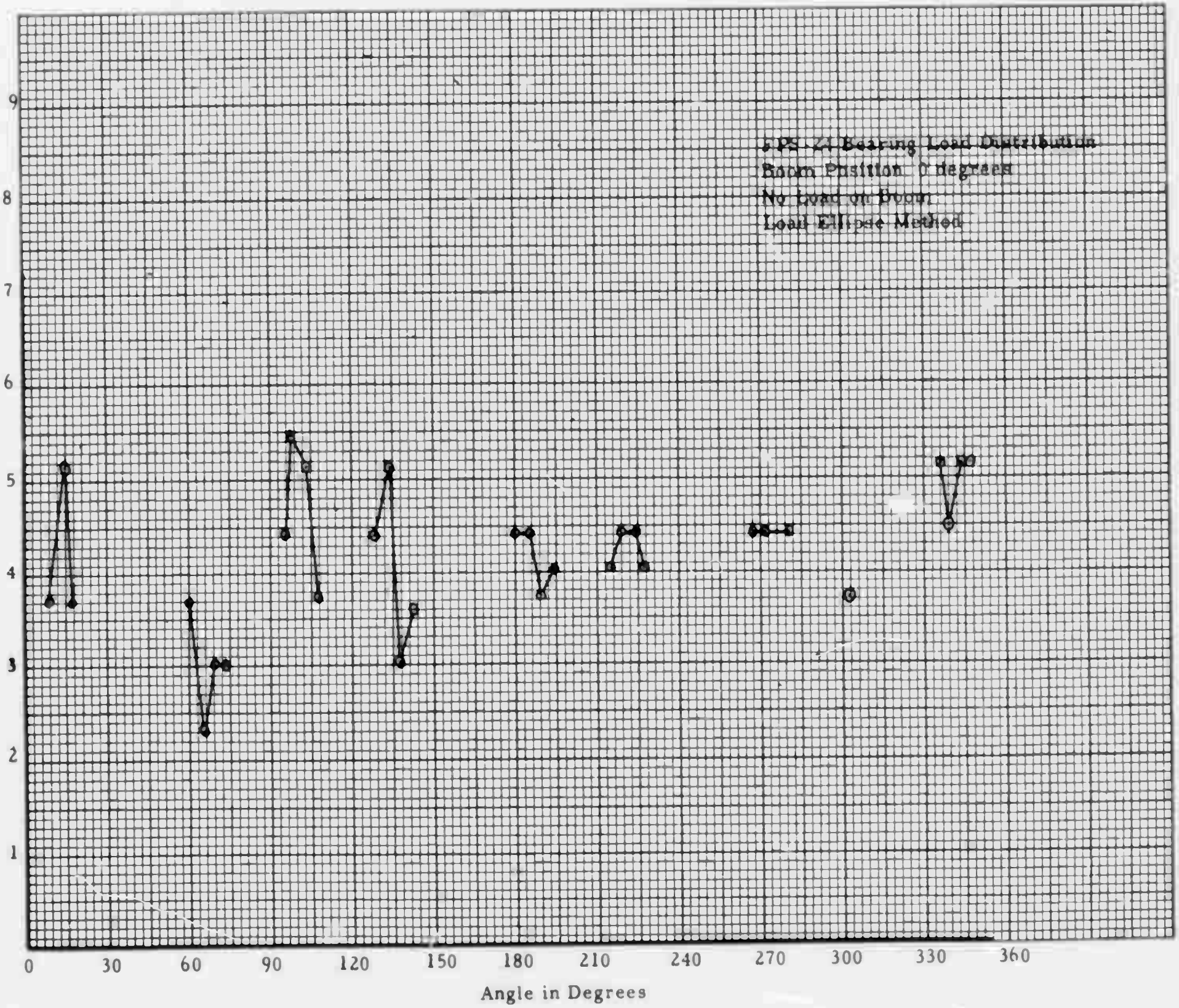

Curve No. 5

15

Date 1-12-65

Condition 3000 # Load

Remarks

Position	Wind Velocity	Wind Direction	Load Angle	Load Major	Load Minor	Contact Ellipse Major	Contact Ellipse Minor
9	0					4400	
15	0					3700	
17	0					5150	Trace
61	0					4050	
65	0					4400	
69	0					4400	
74	0					4400	
95	0					4400	
98	0					4050	
104	0					4050	0
108	0					3700	
128	0					4400	
134	0					4400	
138	0					4400	Trace
142	0					3500	
181	0					4050	
186	0					4050	0
189	0					5150	
194	0					4400	
215	0					4400	
219	0					3700	
224	0					4400	0
228	0					4400	
268	0					4400	
272	0					4400	0
280	0					4400	
302	0					3700	
337	0					3700	
339	0					4400	
344	0					5150	
348	0					5150	

52-53 Flame Gap 74-75 Load Slot

Tabulation No. 6

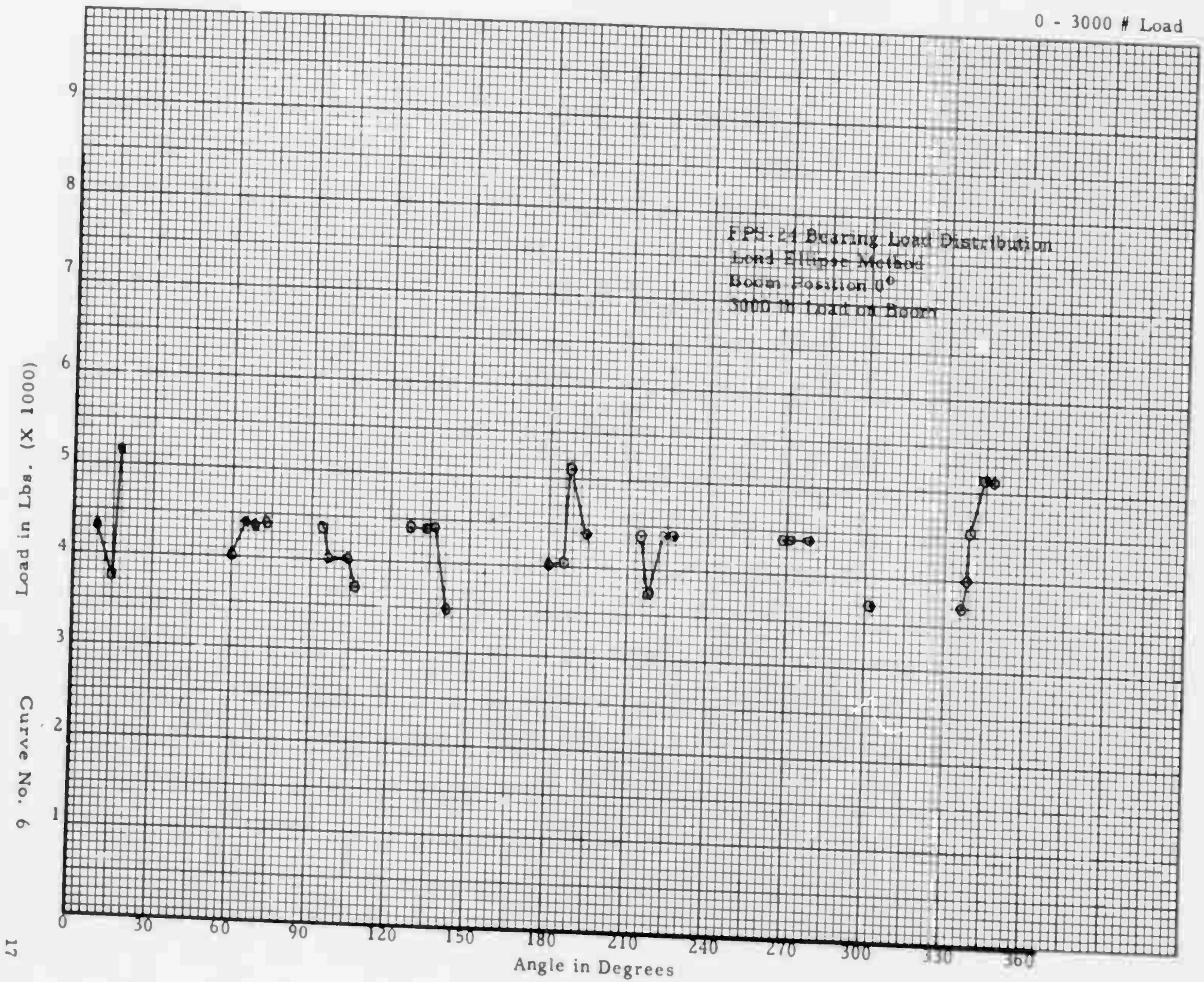
0 - 3000 # Load
EPS-24 Bearing Load Distribution
Load Ellipse Method
Boom Position 0°
3000 lb load on Boom
Load in Lbs. (X 1000)
Curve No. 6
Angle in Degrees
0
30
60
90
120
150
180
210
240
270
300
330
360
1
2
3
4
5
6
7
8
9

Another type of difficulty encountered was the possibility of a gusset coming over the antenna ball slot separator with the antenna in the correct position. There was no solution for this unless a new ball and separator were selected with the probability that the condition might not repeat the next time.

6. Load Ellipse Calibration. Two methods were used to calibrate the loads as obtained with load ellipse technique. The first method consisted of a theoretical calculation of the length of the major axis versus the applied load between the ball and the race. The second method consisted of obtaining actual load ellipse data versus applied load under simulated operating conditions. For this method a section of an FPS-24 bearing and one of the balls was used. The race sections were further modified by machining a 35-degree angle in such a way that a load could be applied by a tensile machine to give proper load angle contact data. With this laboratory setup, the tin plate on both inner and outer races was used and loads were applied to the azimuth bearing section. From this test it was possible to obtain load ellipse major axis length versus load for all loads over the range anticipated for possible operating conditions. This data is plotted on Curve 7.

Both methods for obtaining this calibration data correlated quite closely. The results are based on the actual tests made in the laboratory.

7. Load Cell Calibration. To calibrate the static load cells, strain measurements were obtained versus tensile machine applied load for a range from 0 to 10,000 pounds. With this information, a known load was applied to a section of the azimuth bearing races with two balls and the load cell in place. This data is plotted on Curve 8. From this information of load readout versus applied load and the known ratio of load shared by the load cell itself, the calibration Curve 9 was obtained.

Because of the difficulty in the difference of length of the two load cells, it was necessary to modify one of the load cells and make additional rechecks at Oakdale. This modification consisted of adding 0.002 inch to the length of one of the cells and recalibrating. Calibration data for three load cells is shown. Field data was obtained with each of the three load cells and is shown plotted on Curves 1 and 2.

Date March 29, 1965
March 30, 1965
March 31, 1965

Boom Position 0 Degrees

Condition No Load

Remarks Temperature Differential Tests

Position	Wind Velocity	Wind Direction Rel. to Boom	Load Angle	Load Major lbs.	Load Minor	Contact Ellipse Major	Contact Ellipse Minor
189	10	E	35	3500	-		
March 29							
	Outside temperature 47.5° F		)				
	Inside temperature 61.5° F		) 4:30 PM			ΔT_1 =	14° F
189	10	E-SE	35	3250	-		
March 30							
	Outside temperature 25° F		)				
	Inside temperature 48° F		) 8:00 AM			ΔT_2 =	23° F
						ΔL =	250 lbs.
			$\frac{\Delta L}{\Delta T_2 - \Delta T_1}$ =	250 lbs. / 9° F			
166	9	E-SE	36	3600	-		
March 30							
	Outside temperature 34.5° F		)				
	Inside temperature 56° F		) 6:40 PM			ΔT_1 =	21.5° F
166	11	S	36	3510			
March 31							
	Outside temperature 20.5° F		)				
	Inside temperature 48.0° F		) 8:00 AM			ΔT_2 =	27.5° F
			$\frac{\Delta L}{\Delta T_2 - \Delta T_1}$ =	90 lbs. / 6° F			

Tabulation No. 7

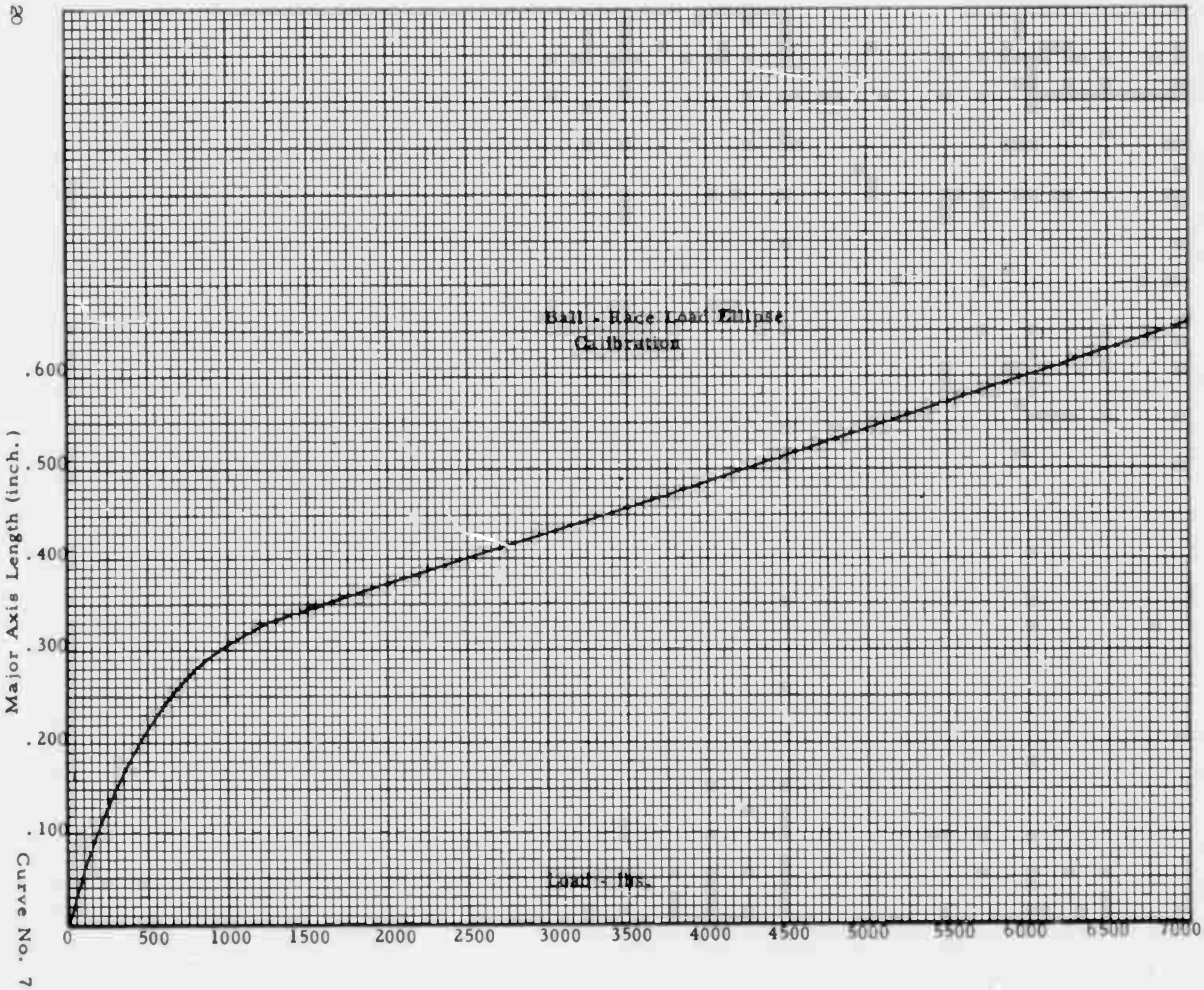
Ball - Race Load Ellipse
Calibration
Major Axis Length (inch.)
.600
.500
.400
.300
.200
.100
0
500
1000
1500
2000
2500
3000
3500
4000
4500
5000
5500
6000
6500
7000
Load - lbs.
Curve No. 7

Date March 29, 1965
March 30, 1965
March 31, 1965

Boom Position 0 Degrees

Condition No Load

Remarks Recheck of original data

Position Ball Number	Wind Velocity	Wind Direction Rel. to Boom	Load Angle	Load Major lbs.	Load Minor lbs.	Contact Ellipse Major	Contact Ellipse Minor
45	10	E	35 Major	3410	0	Load Cell #2	
						March 29	
45	10	E	35 Major	3500	0	Load Cell #3	
						March 30	
43	10	E-SE	35 Major	3600	0	"	"
49	8	E-SE	34 Major	3880	0	"	"
54	15	E-SE	33.5 Major	5300	0	"	"
50	11	E-SE	33.5 Major	5300	0	"	"
49	12	E-SE	34 Major	4050	0	"	"
40	9	E-SE	36 Major	3700	0	"	"
56	10	S	35 Minor	-	1240	March 31	
57	8	S	35 Minor	-	1400	"	"

Tabulation No. 8

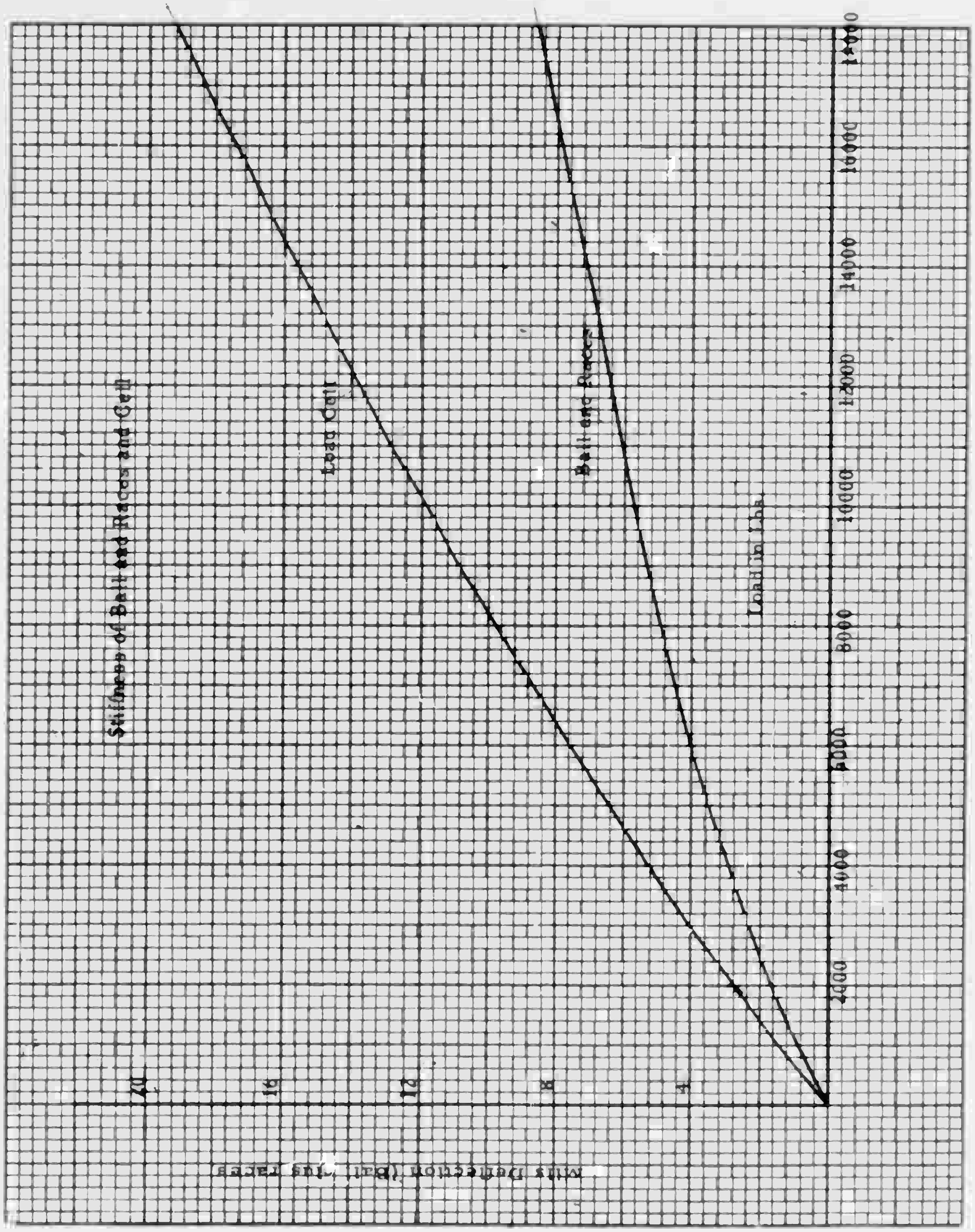
Stiffness of Ball and Races and Cell
Load Cell
Ball and Races
Load in Lbs.
2000
4000
6000
8000
10000
12000
14000
4
8
12
16
20

Curve No. 8

Date March 31, 1965

Boom Position 0 Degrees

Condition 2600 lb. on Boom

Remarks Recheck of original data

Position Ball Number	Wind Velocity	Wind Direction Rel. to Boom	Load Angle	Load Major lbs.	Load Minor lbs.	Contact Ellipse Major	Contact Ellipse Minor
40	10	S	Major 35.5	3500	1400		Load Cell #3
41	10	S	35.Minor		1110		" "
45	10	S-SE	35.Minor		1240		" "
51	9	S	35 Minor		1400		" "
52	8	S	35 Minor		2350		" "
56	10	S	35 Minor		1720		" "

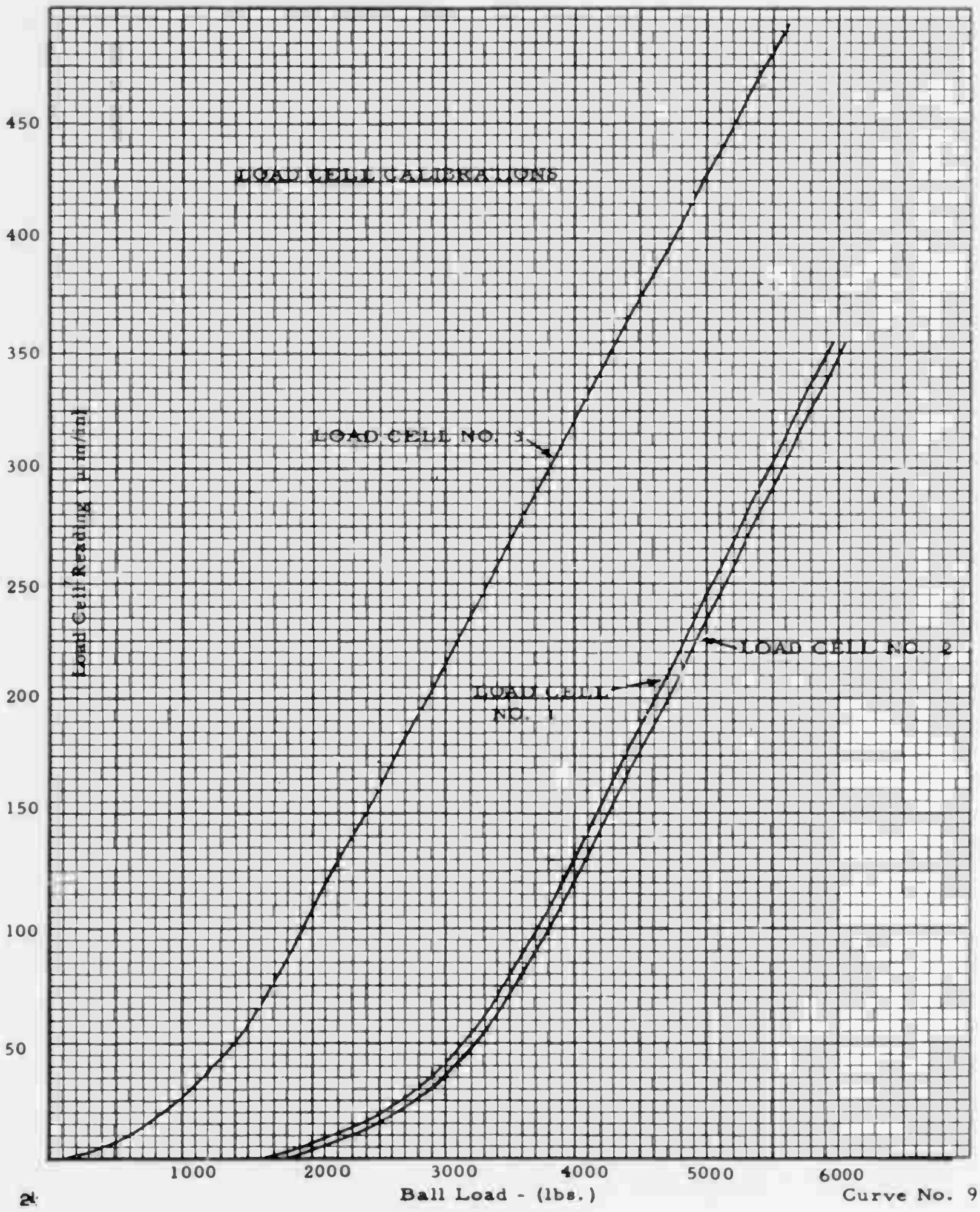
LOAD CELL CALIBRATIONS
LOAD CELL NO. 3
LOAD CELL NO. 2
LOAD CELL NO. 1
Load Cell Reading (μ in/in)
450
400
350
300
250
200
150
100
50
1000
2000
3000
4000
5000
6000
Ball Load - (lbs.)

Curve No. 9

8. Wind Effect. In general, the winds encountered for the full duration of the tests were in the range of 10 to 15 miles per hour from the third quandrant direction. Therefore, little information as to change in wind conditions or effect was obtained. However during the very early stages of the test, information was obtained for one azimuth location with winds varying from 15 to 40 miles per hour. This azimuth location was at 138 degrees relative to the boom and 180 degrees to the direction of the wind. An attempt was made to record data only when the wind velocity had persisted for sufficient length of time to give a uniform effect for the whole antenna. All data obtained represents the direct change in load because the load cell remained in place for all the data taken.

Unfortunately, however, at no time was it possible to obtain any data for a zero wind velocity. Therefore, it was difficult to assign an absolute value to the effect of wind under these wind velocity variations. Only the differences between the conditions are factual.

Some indication of the effect of wind or over- tipping moment can be obtained from the recheck data where one condition at Ball Position 40 data was obtained as the load changed where 2600 pounds were added to the boom.

SECTION B. DYNAMIC LOAD CELL DISCUSSION

9. Introduction. In that the true objective on the FPS-24 bearing overall problem can best be attained by knowing actual dynamic loading conditions within the bearing, considerable thought has been given to a technique permitting this type of measurement. It appeared that it might be possible to use the actual operating ball itself as a load cell. By previously determining the characteristics of deformation of the ball, and then measuring this deformation under operating conditions, it would be possible to actually indicate loading within the bearing.

10. Design. The space permitted for using a dynamic "piggy-back" ball caliper consisted of 1-1/2 inches between the inner and outer race and part of the 13/16-inch separator between each of the balls. Within this space, a gage containing four LVDT's was located. The four LVDT's were located within the gage frame with as much wheel base as possible.

FPS-24 AZIMUTH BEARING

BALL DIAMETER CHANGE

WITH 7000-POUND LOAD

Cage Angle	Pickup Angle	Pickup Number	Division Change	μ inches
39	29	2-4	24.0	- 52.8
	49	1-3	5.5	+ 12.1
42	32	2-4	16.5	- 36.3
	52	1-3	9.5	+ 20.9
47	37	2-4	9.25	- 20.3
	57	1-3	12.0	+ 26.4
52	42	2-4	1.0	- 2.2
	62	1-3	14.0	+ 30.8
57	47	2-4	4.0	+ 8.8
	67	1-3	15.5	+ 34.1
65	55	2-4	10.5	+ 23.1
	75	1-3	16.0	+ 35.2
75	65	2-4	16.0	+ 35.2
	85	1-3	12.0	+ 37.4
80	70	2-4	18.2	+ 40.0
	90	1-3	16.25	+ 35.7
90	80	2-4	17.0	+ 37.4
	100	1-3	18.0	+ 39.6

Tabulation No. 10

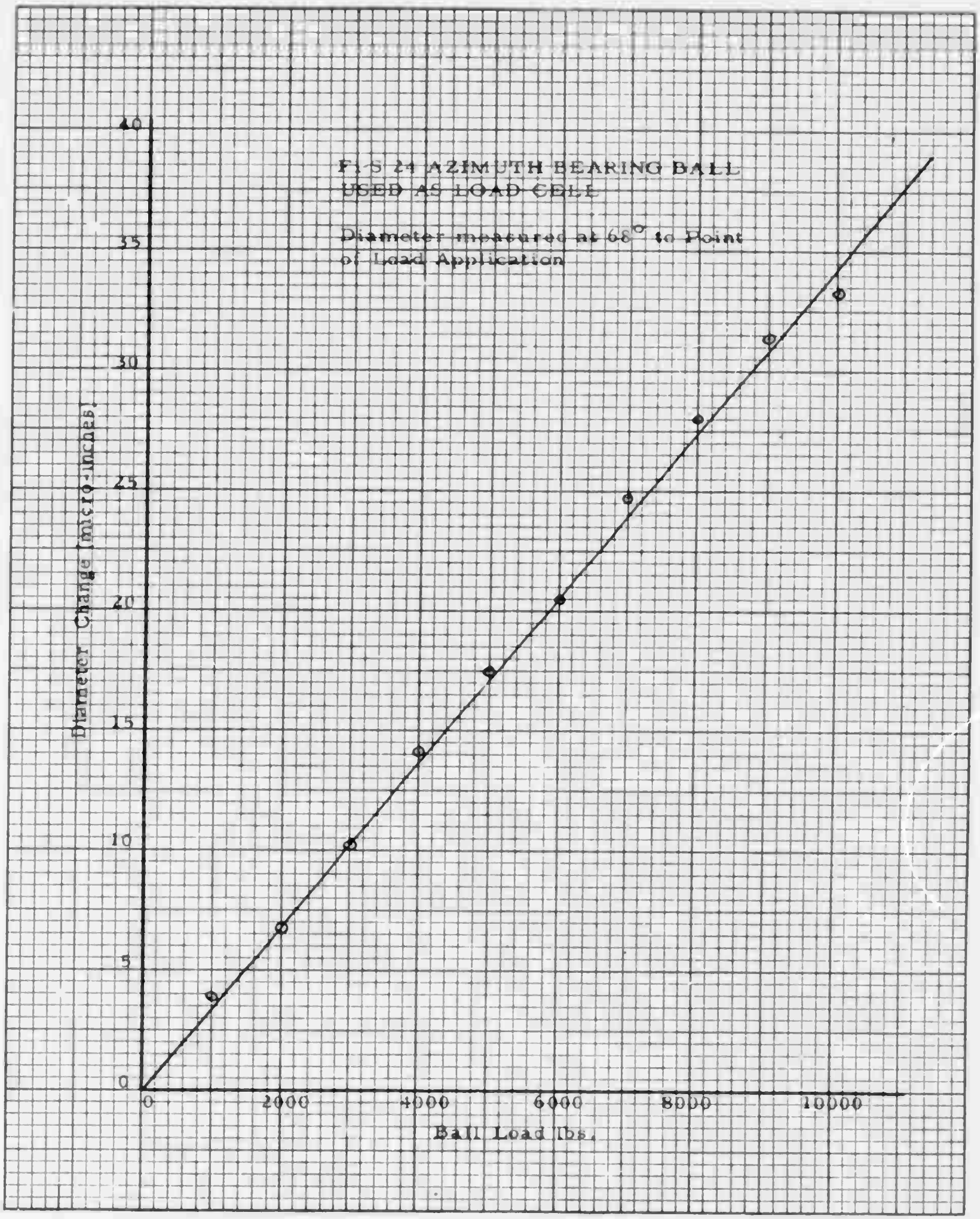
F.S 24 AZIMUTH BEARING BALL
USED AS LOAD CELL
Diameter measured at 68° to Point
of Load Application
Diameter Change [micro-inches]
40
35
30
25
20
15
10
5
0
0
2000
4000
6000
8000
10000
Ball Load lbs.

Curve No. 10

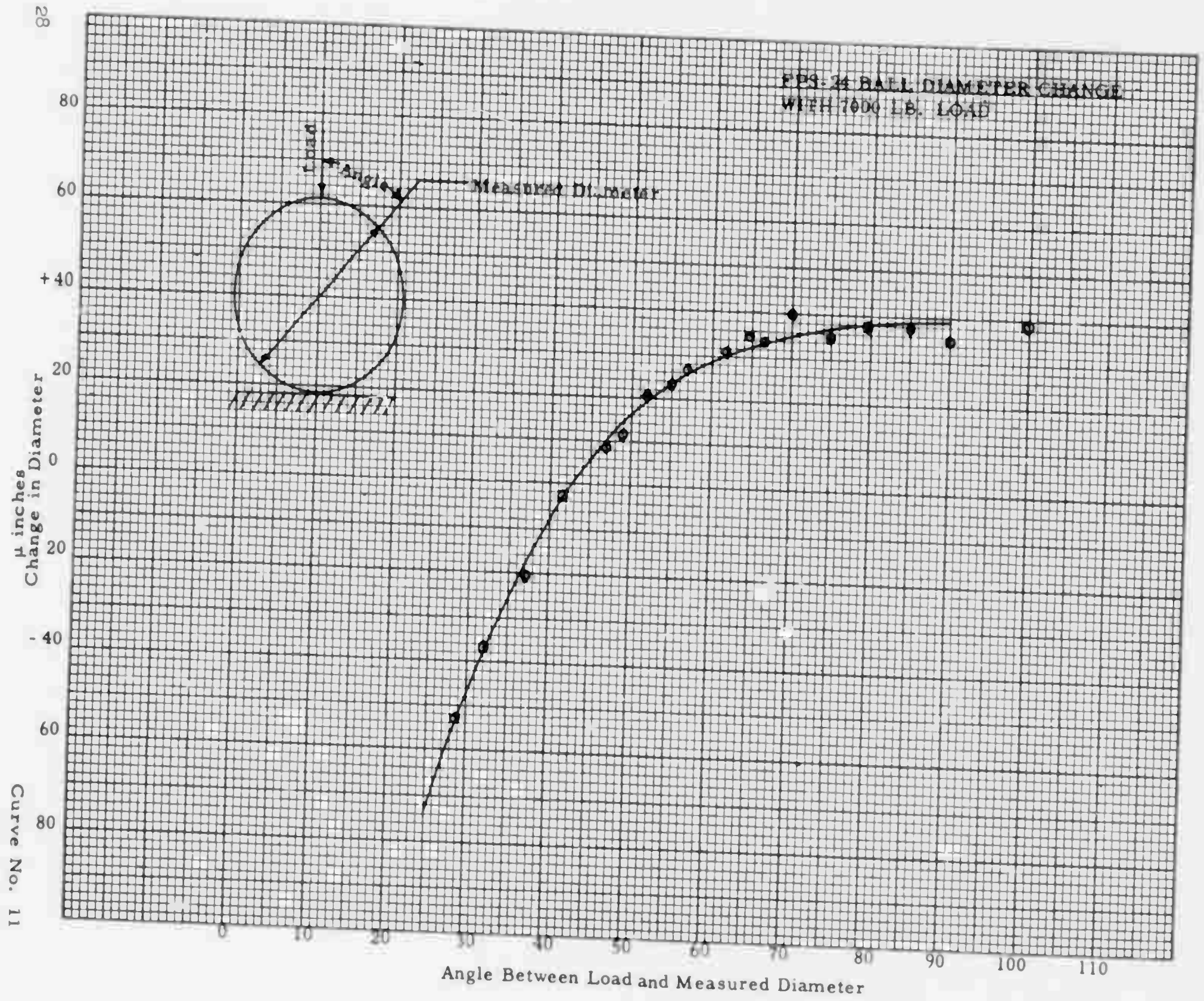
EPS-24 BALL DIAMETER CHANGE
WITH 1000 LB. LOAD
Load
Angle
Measured Diameter
Curve No. 11
μ inches
Change in Diameter
80
60
+40
20
0
20
40
60
80
0
10
20
30
40
50
60
70
80
90
100
110
Angle Between Load and Measured Diameter

Electrically the LVDT's were connected in pairs to measure ball diameter while cancelling any relative movement of the caliper gage containing the measuring elements. Two separators and keepers were modified to permit this gage caliper to be fitted around the ball. The modification in no way altered their basic function as separators and ball space maintainers. These two separators were further supported by a 1-1/4-inch by 3/4-inch curved steel bar connecting the complete two-separator assembly into one rigid structure.

The caliper gage was designed to ride "piggy-back" on the ball itself and register with fixed referenced points against the inner race. Refer to Figure 2 for a pictorial representation of this device.

11. Calibration Data. By loading a standard FPS-24 ball bearing ball in the tensile machine with the caliper and ball placed in the correct relative position, data was obtained on deformation versus applied load. This data is plotted on Curve 10.

12. Ball Deformation Data. To further determine data on deformation of the ball, a bearing ball diameter was measured at many angles relative to the load position. This data is plotted on Curve 11. Examination of this information indicate best location of the LVDT's for diameter measurement. As noted from this curve, the diameter of the ball at an angle of 43 degrees relative to the application of the load showed no change in diameter regardless of the load applied. This made it possible to separate minor axis and major axis loads when applied to the ball under operating conditions. Both transducers were located approximately 43 degrees and 67 degrees with respect to the position of load application for either the major or minor axis of load. In other words, one diameter-measuring set of LVDT's will measure the major axis load and indicate zero for any minor axis load that may be present. The second set of transducers will indicate minor axis load with zero indication of any possible major axis load.

13. Predicted Information. Because of space requirements, the transducers are not mounted radially to the ball; thus, it is possible that any relative movement of the gage with respect to the ball will have some effect. By fixing the face of the measuring transducer normally to the ball surface, some movement will be permitted without

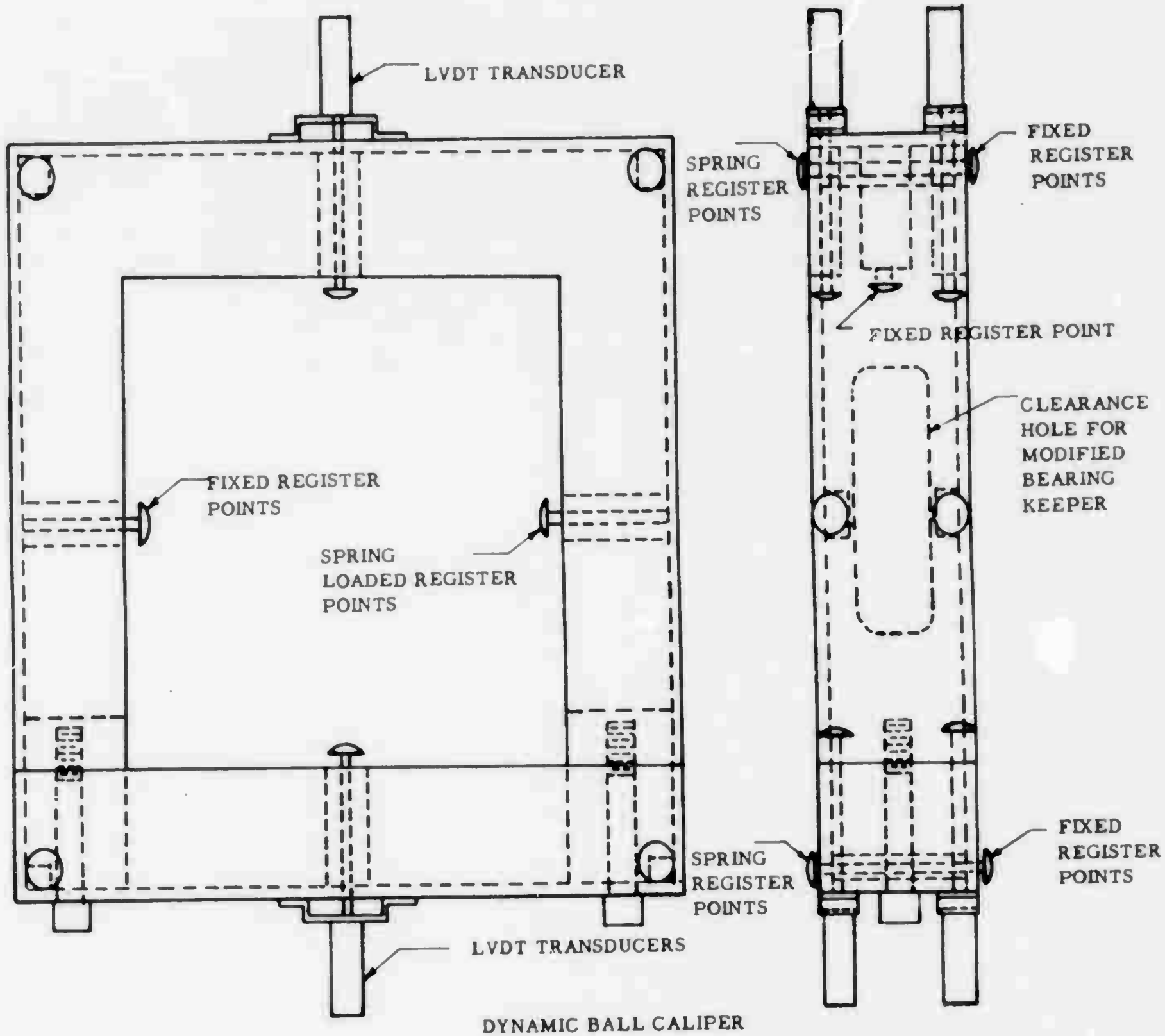

DYNAMIC BALL CALIPER
FIGURE 2

significant indication from the transducer. It is also possible that there will be some slight chatter in the trace of the recording because of the stubbing action of the transducer contact on the ball surface. Laboratory tests have indicated some of this effect, but, in general, the basic curve contains the true and desired information. Therefore, it will be possible to obtain two simultaneous traces with one trace indicating only major axis load and the second trace indicating only minor axis load.

14. Operation Calibration Data. Calibration data was obtained in the laboratory on a tensile machine, as noted in Curves 10 and 11. This calibration will hold for dynamic operating conditions, except that it will be difficult to recheck after leaving the laboratory. However, because of the construction of the FPS-24 bearing, a check calibration can be obtained for every revolution of the bearing. This calibration data will evolve from two sources of information; 1) integration of load for a revolution will equal the total load of the antenna itself, and 2) each time that the ball in use as a load cell passes through the flame gap, both transducers will indicate a zero load. From these two values, the dynamic calibration of the system may be ascertained.

15. Angle of Load Contact Data. The information as to the angle of load contact of either the major or minor axis will become quite difficult to observe in the presence of major and minor axis load indication. It may be possible, after some experience in the field, to obtain some indication of the dynamic contact angle under a condition where only major axis load is known to be present. The sensitivity of the nonindicating transducer to change in load angle is approximately 800 pounds per degree of load angle change. Therefore, when it is assured that no minor axis load is present, it will be possible to define some dynamic load angle indication information.

16. Ball Uniformity. A dynamic measuring system depends upon uniformity of the diameter of the ball itself. In laboratory tests good repeated measurements were taken at varied diameters around the ball, thus indicating there should be no difficulty with a false readout resulting from nonuniform ball diameter.

17. Feasibility. From the laboratory tests performed to date, all indications are that it will be possible to obtain good continuous dynamic data using the dynamic measuring system. With the present instrumentation sensitivity and stability, there should be no difficulty in reading loads as light as 100 pounds. The information on load angle and smoothness of trace will not have as high a quality as desired. Using a cable about 40 feet long will permit us to obtain dynamic data for approximately three revolutions of the antenna at the 5 rpm speed, assuming that the rotary joint is in place. With the rotary joint dismantled (during bearing change) it should be possible to obtain 10 or 15 revolutions at 5 rpm per continuous trace.

18. Mechanical Difficulties at Oakdale. During the original tests at Oakdale, it was determined that it was impossible to use the calipered gage because of lack of clearance with the gussets directly below the bearing. During the second recheck period, sufficient down time would not permit field test of this equipment. At present, the equipment itself has been modified, permitting clearance greater than that required at Oakdale, and it should give no trouble at either Malmstrom or Baudette.

SECTION C. RESULTS

All load distribution measurements for the four conditions of tests are shown on the attached curves and tabulations. A list of this data is shown below:

Curves	
1	FPS-24 Bearing Load Distribution Boom Position 0 Degrees No Load on Boom
2	FPS-24 Bearing Load Distribution Boom Position 0 Degrees 3000-Pound Load on Boom
3	FPS-24 Bearing Load Distribution Boom Position 315 Degrees No Load on Boom
4	FPS-24 Bearing Load Distribution Boom Position 315 Degrees 3000-Pound Load on Boom

5	FPS-24 Bearing Load Distribution Boom Position 0 Degrees No Load on Boom Load Ellipse Method
6	FPS-24 Bearing Load Distribution Load Ellipse Method Boom Position 0 Degrees 3000-Pound Load on Boom
7	Ball - Race Load Ellipse Calibration
8	Stiffness of Ball and Races and Cell
9	Load Cell Reading (μ in/in)
10	FPS-24 Azimuth Bearing Ball Used As Load Cell
11	FPS-24 Ball Diameter Change With 7000-Pound Load

Tabulations

1	FPS-24 Load Distribution Load Cell Method No Load 0 Boom Position
2	FPS-24 Load Distribution Load Cell Method 3000-Pound Load 0 Boom Position
3	FPS-24 Load Distribution Load Cell Method 315-Degree Boom Position No Load
4	FPS-24 Load Distribution Load Cell Method 315-Degree Boom Position 3000-Pound Load
5	FPS-24 Load Distribution Load Ellipse Method 0 Boom Position No Load
6	FPS-24 Load Distribution Load Ellipse Method 0 Boom Position 3000-Pound Load
7	FPS-24 Load Distribution 0 Boom Position Temperature Effect Tests No Load

8	FPS-24 Load Distribution Load Cell Method 0 Boom Position No Load Recheck of Original Data
9	FPS-24 Load Distribution Load Cell Method 0 Boom Position 2600-Pound Load Recheck of Original Data
10	FPS-24 Azimuth Bearing Ball Diameter Change With 7000-Pound Load
11	Static Data Summary

During the recheck of the minor axis load, it was possible to obtain some appreciation for the effect of exact boom position on the variation in loads. There are two points plotted for Ball Position 49 on Curve 1, which indicates that it is possible to obtain a significant variation in indicated load when the boom position varies three to four degrees. The accuracy criteria for location of the boom for the test data was plus or minus five degrees. This tolerance was permitted in order to increase the possible volume. A movement of five degrees in one direction or another would permit removing a separator and allow an additional data point.

A comparison of the loads obtained by the load ellipse method versus the load cell technique shows good correlation. The static load recheck data is shown on Tabulations 8 and 9.

19. Summary and Comments. A summary of the data contained in Tabulations 1, 2, 3, 4, 5, and 6 is shown in Tabulation 11. This tabulation shows the high, low, and average ball load based on the aforementioned tabulations. It can be seen that close correlation exists between the "Load Cell" method and "Contact Ellipse" method. Average ball load for the no load condition is approximately 4220 pounds. Using this average ball load and a contact angle of 35 degrees, the total load on the bearing is approximately 203,448 pounds. It should be noted that this figure is approximate and that a more accurate figure is presented in the data contained in the life estimate analysis section of this report.

Refinement of the data will take into account actual distribution, actual contact angle, and minor load.

Tabulation 7 presents the data obtained under different ambient temperature conditions. This data indicates that while a minor change in load occurs, due to a temperature differential, it is not significant enough to effect any substantial change in loading calculations.

SECTION D. FIELD TEST OF DYNAMIC BALL CALIPER

20. Field Installation. Some difficulties were encountered in the installation of our required separators and ball caliper cage.

a. In general, they were as follows:

1. The separator teeth were machined about 1/16 inch on the face of each tooth. This modification, in effect, permitted greater random spacing between balls. As a result, the two separators with normal size teeth would not fit between all balls without the considerable work of moving the balls to the proper spacing.

2. Closely related to the first difficulty, the two separators had to be exactly spaced with respect to each other to permit freedom of the calipered-ball cage and the installation of the support connecting the two separators.

3. Because of the installation of the bearing immediately preceding the field test, it was possible to grind any necessary obstructions that might cause trouble through lack of clearance with the LVDT's. There was one slight additional difficulty, noted later in our tests, as a result of the clearance problem, showing up as a magnetic proximity and having the effect of putting pulses in the readout system each time a transducer was directly over a gusset.

b. Several other anticipated difficulties were greatly reduced in magnitude from our laboratory estimates. These were as follows:

1. Since it was necessary to adjust the mechanical position of the LVDT's on the bottom of the cage from outside of the turret, with the readout system inside the

turret, it was anticipated that this would create some problems. In actual field tests, however, with only voice signaling between two personnel, it was fairly easy to adjust the bottom two transducers within microinches of the correct location.

2. The rotary joint was not assembled in this installation; hence it was very easy to obtain 20 to 30 revolutions of 5-rpm data. No special sacrifice wire technique was necessary, and, in the event that additional data should be required, it would only be necessary to disconnect leads from the amplifier and untwist the leads to their original position.

21. Operation. The first data was taken at 1/4 rpm-CW until the transducers passed the flame gap on the outer race. The antenna was then returned to its original position where the transducers could be visually inspected. No damage was noted and traces indicated excellent results. In fact, the traces themselves were mirror images between CW and CCW movements.

The second data obtained was for one full revolution of 1/4 rpm. Following this run, inspection indicated that the transducers had come in contact with a gusset resulting in broken leads and severe damage to the main installation on the bottom of the transducer. A quick electrical check indicated that the only damage was external and could be repaired by reconnecting the broken leads. The repairs were performed and, in the process, the remainder of the damaged installation was removed and approximately another 1/8 inch clearance was obtained. With this modification, 360 degrees rotation was obtained without further interference or damage to the transducers. With the transducer returned to the caliper cage, data was obtained both at 1/4 rpm and approximately 30 revolutions at 5 rpm, including slowdown and static data with only the wind gusting between 15 and 20 miles per hour.

A review of this data indicated little stubbing or chattering between the transducer tip and the ball. It showed the predicted separation between major and minor axis loads. The 5-rpm data indicated only a low percentage of minor axis load per revolution with a slight indication that a few light loads were present for the greater portion of a revolution. the angle of contact is a doubtful piece of information from the data. It may be possible after some significant testing and analysis of data to correlate some indication of contact

angle with the very small minor axis loads that were noted in the data. It should be pointed out at this time that two obstacles to good data analysis can be corrected. They are: 1) an indication of hang-up in the follow-up of the transducer, and 2) the false readout as a result of the magnetic proximity of the transducers with magnetic material such as the gussets.

Although determination of exact loads is not an objective here, it is possible to get some indication of variation in load and magnitude based on the zero value obtained at the time the ball runs through the flame gap in the outer race or the load slot in the inner race. To get a good average load it would be necessary to obtain adequate comparison by integrating load for many revolutions to present all possible conditions of wind and any dynamically or statically unbalanced conditions which the antenna must traverse to present all possible conditions for average loading.

22. Results. Our results indicate that the use of such a ball calipered technique is feasible and good dynamic data can be obtained. Both major and minor axis dynamic data are possible with such a system. Also, it will be possible to obtain good indications of load under zero rpm conditions and wind variations. Some load angle contact information is also possible.

23. Recommendations. Good dynamic and static informat on can be obtained with slight modifications of present equipment. Much better dynamic and static data could be obtained by making a significant design change in the cage and separator. This redesign is motivated by need for ease of assembly and use within the bearing. It is recommended that the more extensive modification be performed and a complete program be established to obtain dynamic, static, dynamic balance, and wind data. This data should then be analyzed and supplied to knowledgeable personnel to make computer studies of bearing expected life based on actual maximum load conditions during normal operation of an FPS-24 bearing.

24. Summary and Comments. The operation of the calipered ball device is satisfactory and the data obtained proves feasibility of the device. A review of this data shows some interesting trends which may be expected from wind load, weight location, and bearing ridigity.

This data is preliminary in nature. The assignment of any load values based on a rough calibration would be speculation and possibly misleading. It should be noted that calibration and assignment of absolute values was not part of the feasibility program.

Figure 3 shows data taken at 1/4 rpm over 90^{o} of ball rotation. As expected there is an increase in both major and minor load from the unloaded position (flame gap) to a peak approximately 45^{o} advanced from the no load position and tapering down to lower loadings.

Figure 4 shows data taken at 5 rpm over 360^{o} of ball rotation. This data shows very little minor axis load which is quite constant throughout 360^{o}. The major axis load appears to increase from some average load to a peak load over approximately 180^{o} of ball rotation. The peak itself appears to extend over approximately 50^{o} of rotation.

One set of data was taken at zero rpm to observe the effect of wind only. This is shown in Figure 5 and indicates variation in both major and minor axis loads. The variations appear to be cyclic and occur at a rate of approximately two cycles per second.

The variation in major and minor load from zero to five rpm may possibly be due to a combination of bearing ridigity, weight location, and wind load. These conditions probably have a more pronounced effect on minor axis load at zero rpm where as at five rpm the effects are balanced out from the dynamics of operation. It might be concluded that dynamic balancing would tend to minimize minor axis loads while enhancing a more uniform major load distribution around the bearing. A complete set of dynamic data taken before and after dynamic balancing would be most beneficial and could result in achieving an optimum load distribution.

FIGURE 3

DYNAMIC CALIPER BALL LOAD TEST
1/4 RPM (SCALED DOWN IN TIME)
WIND VELOCITY 14 KNOTS

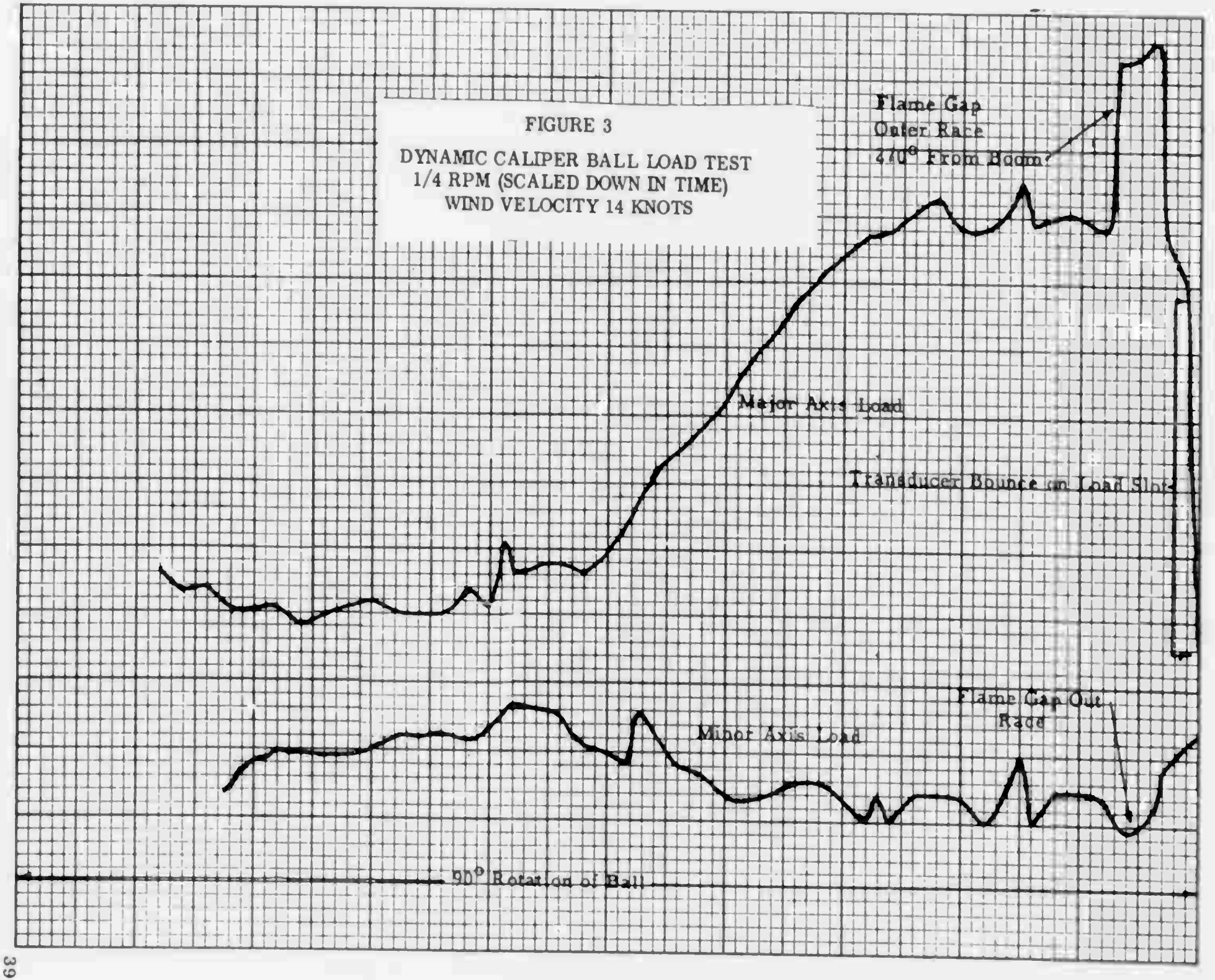

FIGURE 4

DYNAMIC CALIPER BALL LOAD TEST
5 RPM - WIND VELOCITY 14 KNOTS

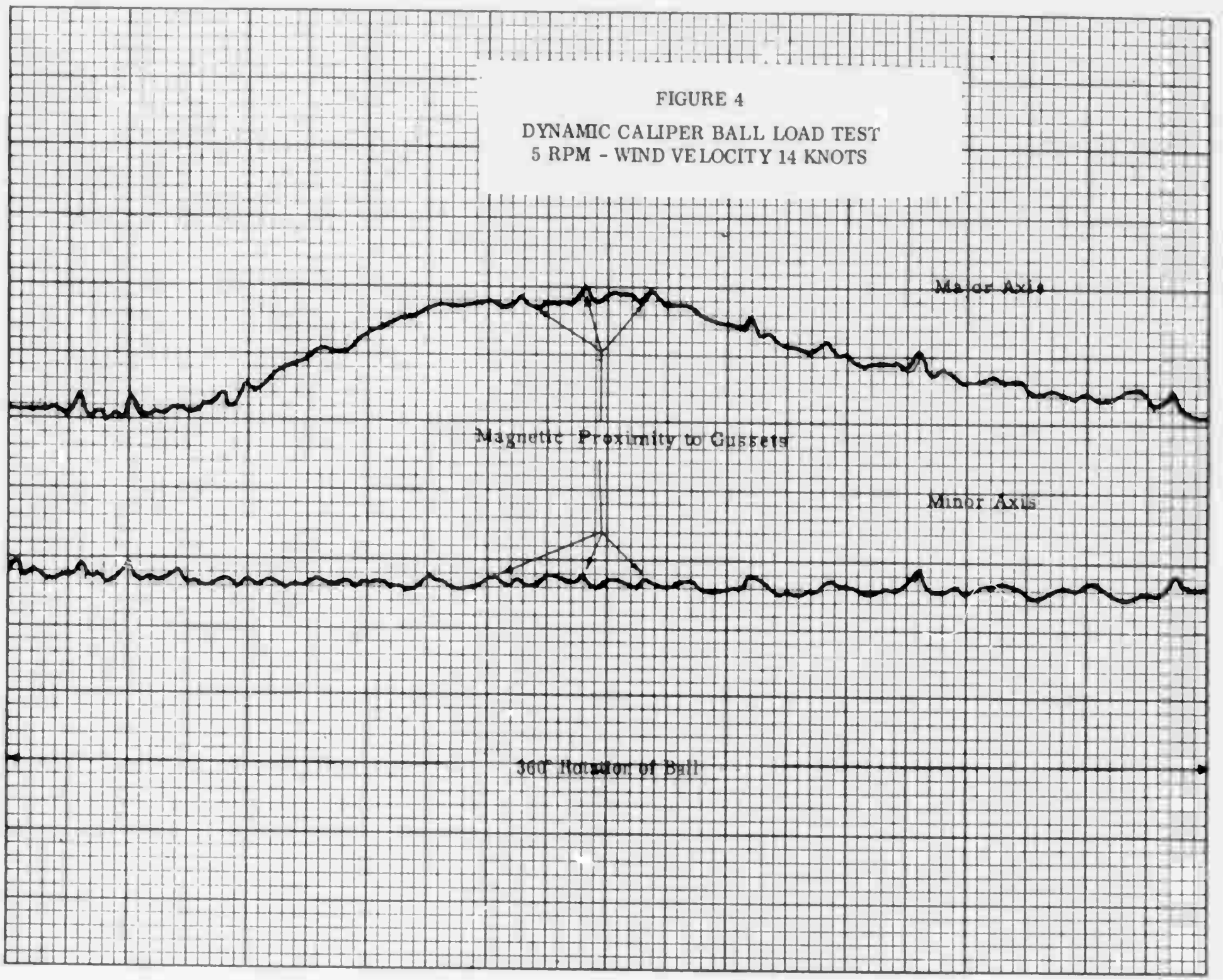

Figure 5,
DYNAMIC CALIPER BALL LOAD TEST
0 RPM - WIND TEST
WIND VELOCITY - 15-20 KNOTS

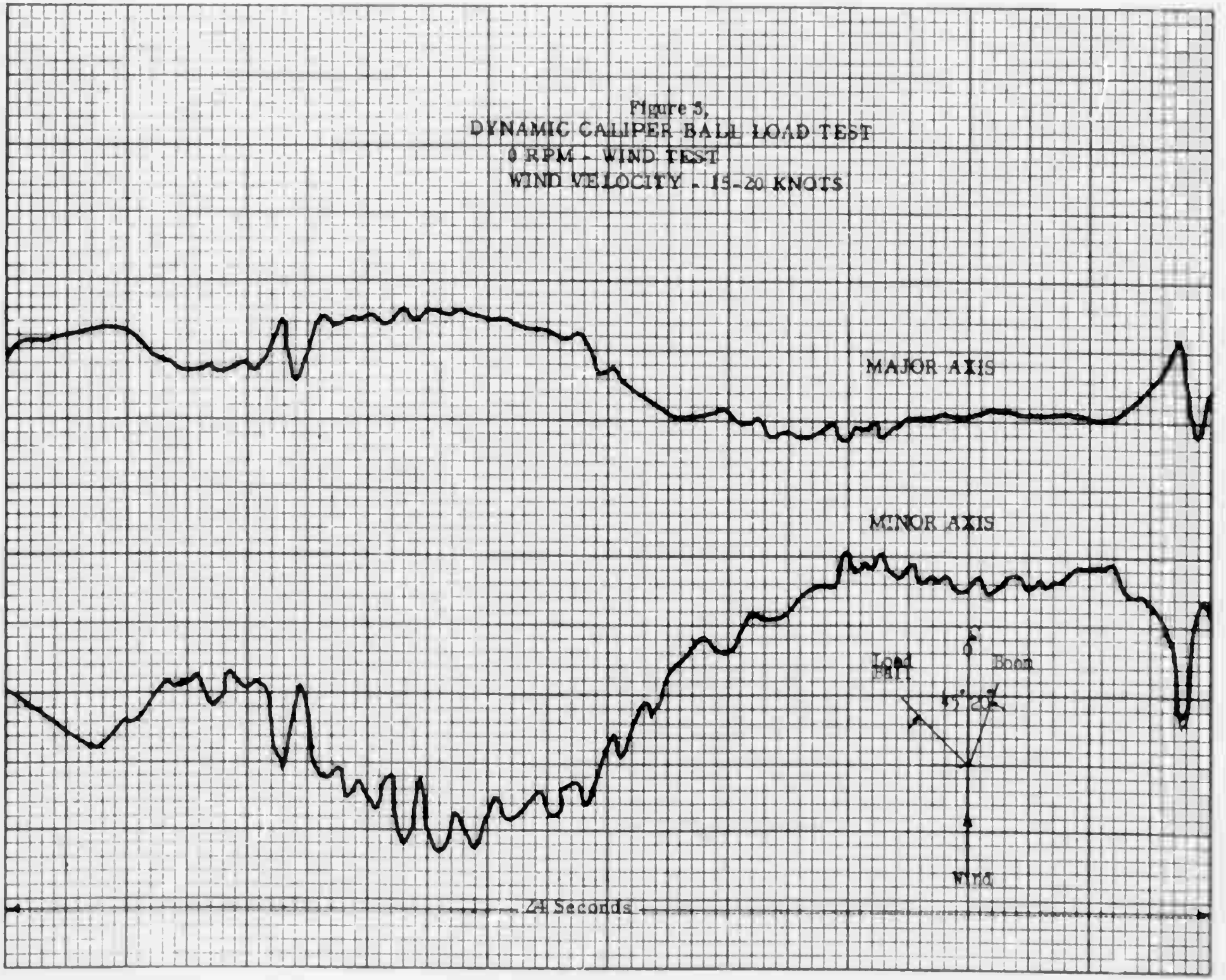

STATIC DATA SUMMARY

Reading	0°-No Load		0°-3000#		315°-No Load	315°-3000#
	Load Cell	Cont. Ellipse	Load Cell	Cont. Ellipse	Load Cell	Load Cell
High	5010#	5450#	5530#	5150#	5070#	4890#
Low	3300#	2300#*	3490#	3500#	3420#	3200#
Average	4183#	4180#	4317#	4298#	4291#	4253#

Note: *Possible error in data taking. Figure believed to be approximately 3000 pounds.

= Pounds

CHAPTER 2

AN EVALUATION OF THE MEASURED LOAD DISTRIBUTION FOR THE AN/FPS-24 ANTENNA BEARING

SECTION A. INTRODUCTION

25. General. The General Electric Electronics Laboratory under contract to the Rome Air Development Center measured the internal load distribution in the rolling element azimuth bearing of the Radar Set AN/FPS-24 Antenna Pedestal. This chapter constitutes an evaluation of this measured load data.

A static equilibrium analysis of the antenna showed that the measurement system did not have sufficient sensitivity to sense the test changes in simulated loading on the boom or the magnitude or direction of the wind loading during test. Within the accuracy of the measurements, there was no significant difference between the life computation based on the measured load distribution and a life computation based on a calculated load distribution for the same loading conditions.

SECTION B. BEARING EXTERNAL LOAD ANALYSIS

26. Bearing Geometry. The antenna bearing of the AN/FPS-24 bearing is a four-point contact ball bearing. Each ball contacts the grooves in each race at two points (Figure 6). Because it has four contact points, the bearing can handle radial, thrust and moment loads, singly or in combination.

27. Bearing Loads. The loads on the AN/FPS-24 antenna bearing are of three types.

a. Weight loads
   (1) Static thrust
   (2) Static unbalance
b. Wind loads
c. Dynamic unbalance

For this analysis the weight of the antenna is taken from the load cell weight measurements reported in Reference 1. These are summarized in Table 1.

TABLE 1

ESTIMATED ANTENNA WEIGHT

Net antenna weight	177,200
Estimated weight of outer race	3,000
Estimated weight of side panels removed under test	1,500
Total weight	181,700 lbs

The static unbalance was taken as 126,400 in-lbs in the direction of the feedhorn.

The wind load was calculated from the empirical equation $F=.004V^2$. The results are summarized in Figure 7. The wind load creates both a radial load and over turning moment. In the calculations, it is assumed that the drag load on the antenna is independent of wind direction.

The net dynamic unbalance was taken as 369,000 in-lbs in the direction of the antenna.

Table 2 is a summary of the AN/FPS-24 bearing loading conditions at 5 rpm. These figures include the net dynamic unbalance.

28. Static Equilibrium Evaluation. Load cell measurements were made for two specific antenna positions.

a. Position (315°) was with the center line of the horn boom positioned as nearly as possible on a line that connects diametrically opposite corners of the pedestal support points.

b. Position (0°) was with 45° rotation from position (315°).

For each of these positions measurements were made with no load on the boom and with 3000 lbs on the boom. Only for the 0° position were complete four-point contact loads taken.

These load conditions are illustrated in Table 3.

TABLE 2

BEARING LOADING CONDITIONS

Operating - Loads applied to outer race. Outer race rotates at 5 rpm. Outer race rotates with respect to the load.

52 knots
60 mph

A. .25% of time

Thrust load	220,000#
Overturning moment	20.8×10^6 in-lbs.
Radial load	63,000#

B. .75% of time

Thrust load	178,000#
Overturning moment	20.8×10^6 in-lbs.
Radial load	63,000#

C. 4.75% of time

Thrust load	220,000#
Overturning moment	5.5×10^6 in-lbs.
Radial load	15,700#

26 knots
30 mph

D. 14.25% of time

Thrust load	178,000#
Overturning moment	5.5×10^6 in-lbs.
Radial load	15,700#

E. 20% of time

Thrust load	220,000#
Overturning moment	1.6×10^6 in-lbs.
Radial load	3,930#

13 knots
15 mph

F. 60% of time

Thrust load	178,000#
Overturning moment	1.6×10^6 in-lbs.
Radial load	3,930#

Non-Operating - survival

Thrust load	178,000#
Radial load	180,000#
Overturning moment	59.5×10^6 in-lbs.

TABLE 3

TEST LOAD CONDITIONS

Case	Boom Position	Boom Load lbs	Avg. Wind Direction	Avg. Wind Velocity	Four Point Loads
1	0^{o}	0	WSW	12.9	Yes
2	0^{o}	3000	SW	10.7	Yes
3	315^{o}	0	WSW	12.1	No
4	315^{o}	3000	SW	10.4	No

If the antenna including the outer race of the antenna is considered as a free body diagram, the equations of static equilibrium must be satisfied, i.e.

$$\Sigma F_x = \Sigma F_y = \Sigma F_z = 0$$

$$\Sigma M_x = \Sigma M_y = \Sigma M_z = 0$$

Figure 8 shows a sketch of the bearing outer race and the coordinate system used. By summing up the ball loads on the outer race, the resultant moment and force on the antenna can be obtained. In order to satisfy static equilibrium, the resultant of the ball loads must equal the imposed loads on the antenna.

In particular, the net radial resultant should be equal and opposite in direction to the wind load. The resultant force in the z direction must equal the antenna weight. The resultant moment must be balanced out by the vector sum of the static unbalance and the wind moment. These calculations serve as a check on the validity of the data. A computer program was written to sum up all of the measured ball loads and to determine the components of their resultant moment and force. This program, called Bearing Data Evaluation Program (BDEP) finds components of the resultant moment and force of the individual ball loads and also calculates the bearing life for the measured ball loads.

Table 4 is a summary of the static equilibrium calculations. Cases 1 and 2 are the two test conditions for which complete load data are available. The components of the imposed loads are shown in comparison with components of the resultant ball loads. In order to satisfy static equilibrium, these respective components should be equal and opposite in direction.

The most obvious check is to see that the summation of the ball loads in the vertical direction equals the antenna weight including the outer race. In Case 1, the resultant of the ball loads in the vertical direction is 7 percent higher than the antenna weight. When an additional 3000 pounds is added to the boom (Case 2), the resultant of the ball loads is one percent lower than the antenna weight plus the boom weight.

This apparent inconsistency can be explained by taking into account a more complete minor load distribution. This is shown in Case 1a of Table #4. A comparison of Case 1a with the antenna weight shows the ball loads in the vertical direction to be only 4% higher. A comparison of Cases 1a and 2 indicates agreement within experimental error. Analyzing Cases 1a and 2 on an equivalent basis gives an average resultant total load of 183,940 lbs. This is within ± 2.6% of the cited values.

The net radial load should be equal to the wind load and be opposite in direction to the wind. If we consider Case 1, the wind was from WSW with respect to the boom.

Referring to Figure 6, R is the resultant of the wind (from Figure 7) R = 3000 lbs F_y is R's projection on the z-axis:

$$F_y = R \times \cos 67.5^{\circ} = 3000 \times 0.3827 = 1150 \text{ lbs}$$

Likewise:

$$F_x = R \times \sin 67.5^{\circ} = 3000 \times 0.9239 = 2770 \text{ lbs}$$

M_w is the moment created by the wind (from Figure 7) $M_w = 1.2 \times 10^6$ in/lb
Resolving M_w at the y and x-axis gives:

$$M_{wy} = M_w \times \sin 67.5 = 1.11 \times 10^6 \text{ in/lb}$$
$$M_{wx} = M_w \times \cos 67.5 = 0.46 \times 10^6 \text{ in/lb}$$

The static unbalance M_s = 126400 in-lb and M_{wx} has the same direction and make the total moment vector along the x-axis equal: M_x = -586400 in-lb with respect to the coordinate system of Figure 5.

The radial resultant of the measured ball loads should give a force of components

$$F_x = -2770 \text{ lb}$$
$$F_y = -1150 \text{ lbs}$$

and an angle of 247.5°. The actual resultants for cases 1, 2, and lb are summarized in Table 5.

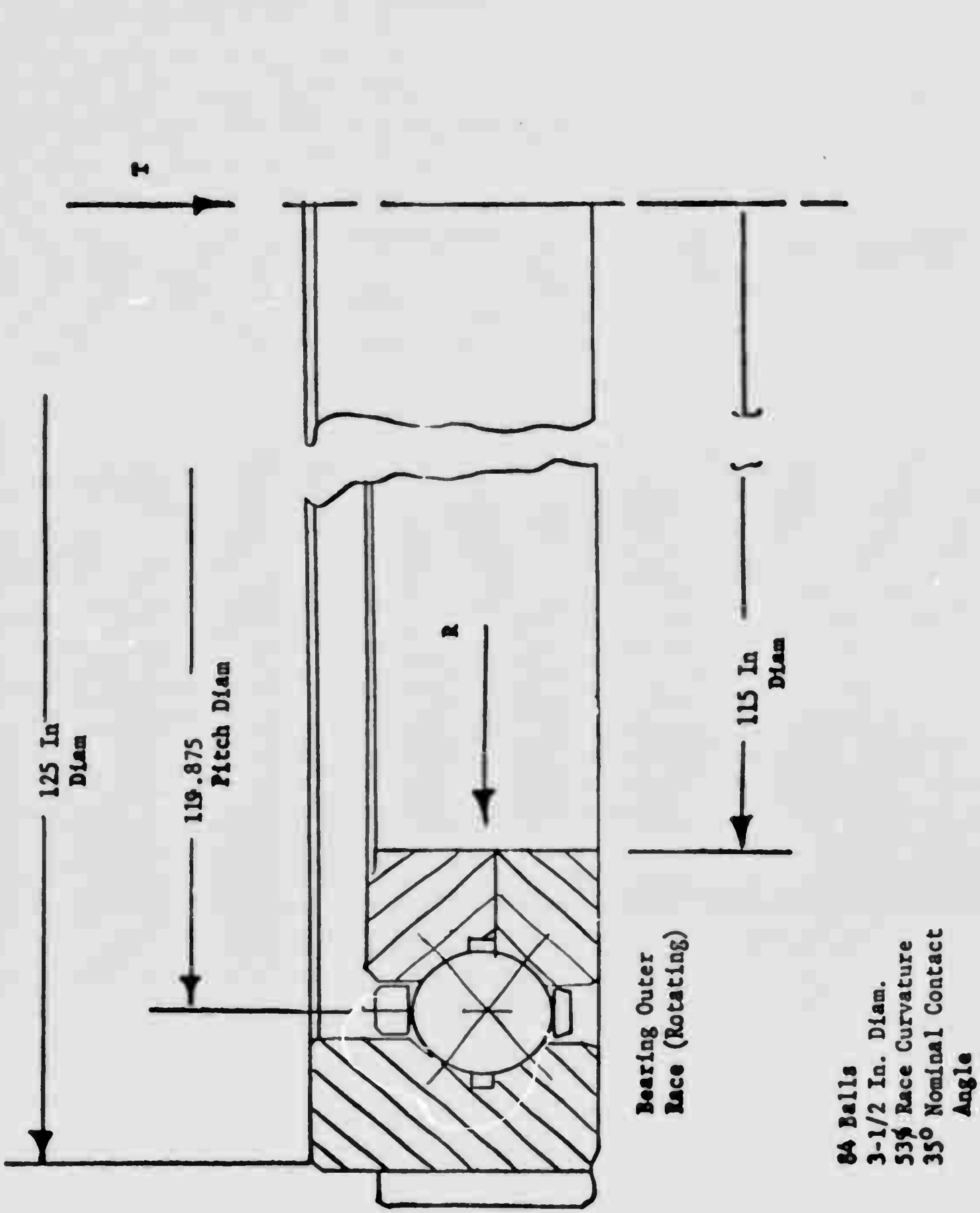

Figure 6. AN/FPS-24 Antenna Bearing (4-point Contact Type)

TABLE 4

STATIC EQUILIBRIUM EVALUATION

Case No.	Load Condition	Imposed Loads						Resultant of Ball Loads					
		F_x lb	F_y lb	F_z lb	M_x in-lb $\times 10^6$	M_y in-lb $\times 10^6$	M_z in-lb $\times 10^6$	F_x lb	F_y lb	F_z lb	M_x in-lb $\times 10^6$	M_y in-lb $\times 10^6$	M_z in-lb $\times 10^6$
1	No boom load, 0^o	2770	1150	-181,700	-.5864	1.11	0	-3860	+6650	194,790	.3802	+.02742	0
2	3000# boom load, 0^o	1554	1554	-184,700	-2.382	.600	0	-1660	-5730	182,040	1.2080	-.6794	0
3	No boom load, 315^o 4 pt from I	2310	956	-181,700	-.5094	.924	0	+453	+4660	199,340	.3800	-.0934	0
4	3000# boom load, 315^o 4 pt from II	1410	1410	-184,700	2.348	.566	0	-14,160	-14,770	182,550	.8249	-.2013	0
1a	Measured two pt loads, calculated 4 pt loads, no preload	Same as #1						-9350	+360	188,840	+.6352	-.19397	0
2a	"	Same as #2						+9970	-12190	178,990	+1.4799	-.2084	0
1b	Measured two pt loads, calculated 4 pt loads, 0.002 in preload	Same as #1						-9910	-700	187,740	+.6799	-.2179	0
2b	"	Same as #2						+9924	-13,710	177,920	+1.544	-.2100	0

TABLE 5

RESULTANT RADIAL LOAD BASED ON MEASURED BALL LOADS

Case	BDEP-Calculated Radial Reactive Force F_y	F_x	Ratio F_y/F_x	Direction of Radial Reactive Resultant (y axis is $\theta = 0$) θ	Calculated Wind Force Direc.	Radial Reactive Force Resultant $F = \frac{F_x}{\cos\theta}$	Meas. Wind Direc.	Wind Force lbs. (Fig. 2)
1	+6650	-3800	-1.72	330^o	150^o	7720	67.5^o	3000
2	-5730	-1660	+3.45	196^o	16^o	6000	45^o	2300
1b	-700	-9910	0.071	266^o	86^o	9930	67.5^o	3200

The wind force direction should be 180^o away from the calculated ball resultant. For Case 1, analysis of the ball loads indicates the wind force 82.5^o away from the actual recorded wind direction. For Case 2, the agreement is much closer with only a 29^o difference between the actual wind direction and that deduced from the ball loads. The wind force deduced from the ball loads ran more than twice the value obtained from the empirical equation of Figure 7.

Table 6 gives the overturning moment and radial components based on ball loads. The residual unbalance moment is known and the radial component is only due to the wind. Table 6 indicates the computation routine and results for Case 1, 2 and 1b.

TABLE 6

RESULTANT WIND MOMENT BASED ON MEASURED BALL LOADS

Case	Static Unbalance M_s (about x)	BDEP-Calculated Total Moment M_y	M_x	Moment Due to the Wind M_{wy}	M_{wx}	Ratio M_{wy}/M_{wx}	Direction of Wind M-vector (y-axis is $\theta = 0$) θ	Calculated Wind Force Direc.	Moment Resultant $M_w = \frac{M_{wx}}{\cos\theta}$
1	-126400	+27420	+380200	-27420	-253800	0.108	264^o	354^o	255000
2	-1782400	-679370	+1207990	+679370	+574410	1.18	40^o	130^o	887000
1b	-126400	-217910	+679870	-217910	-553470	-0.394	292^o	22^o	1510000

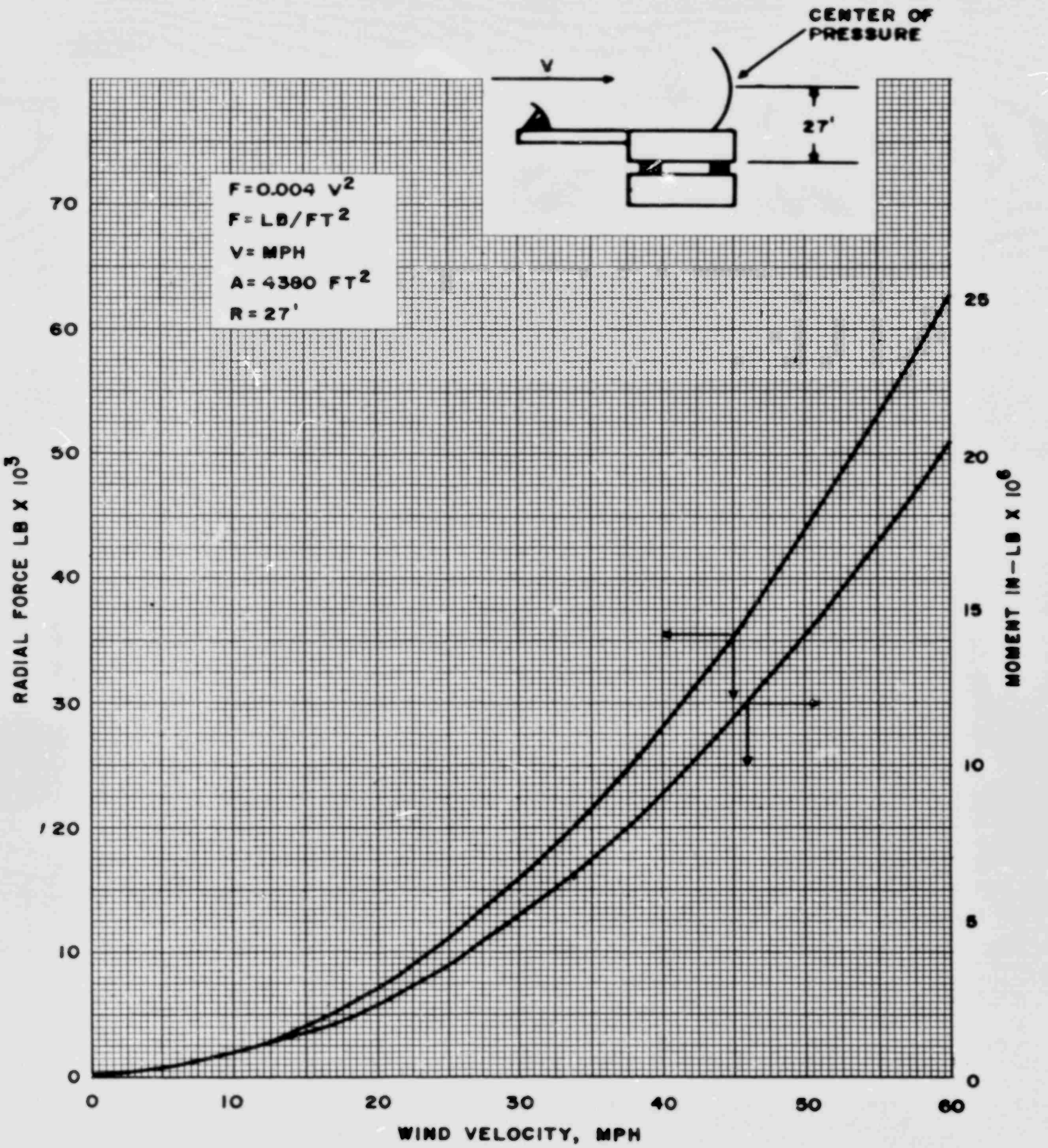

Figure 7. Estimated Antenna Wind Load

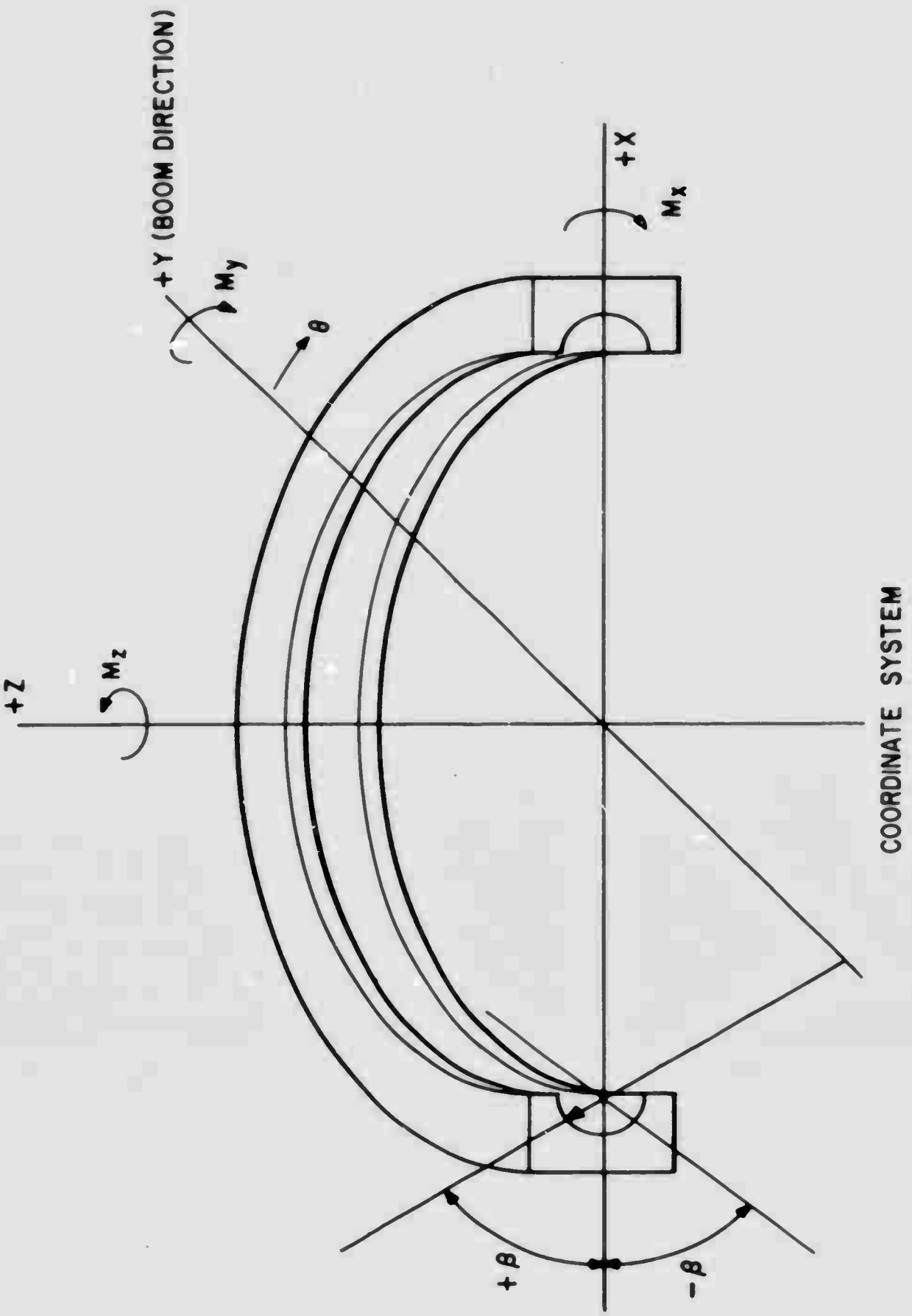

Figure 8. Coordinate System

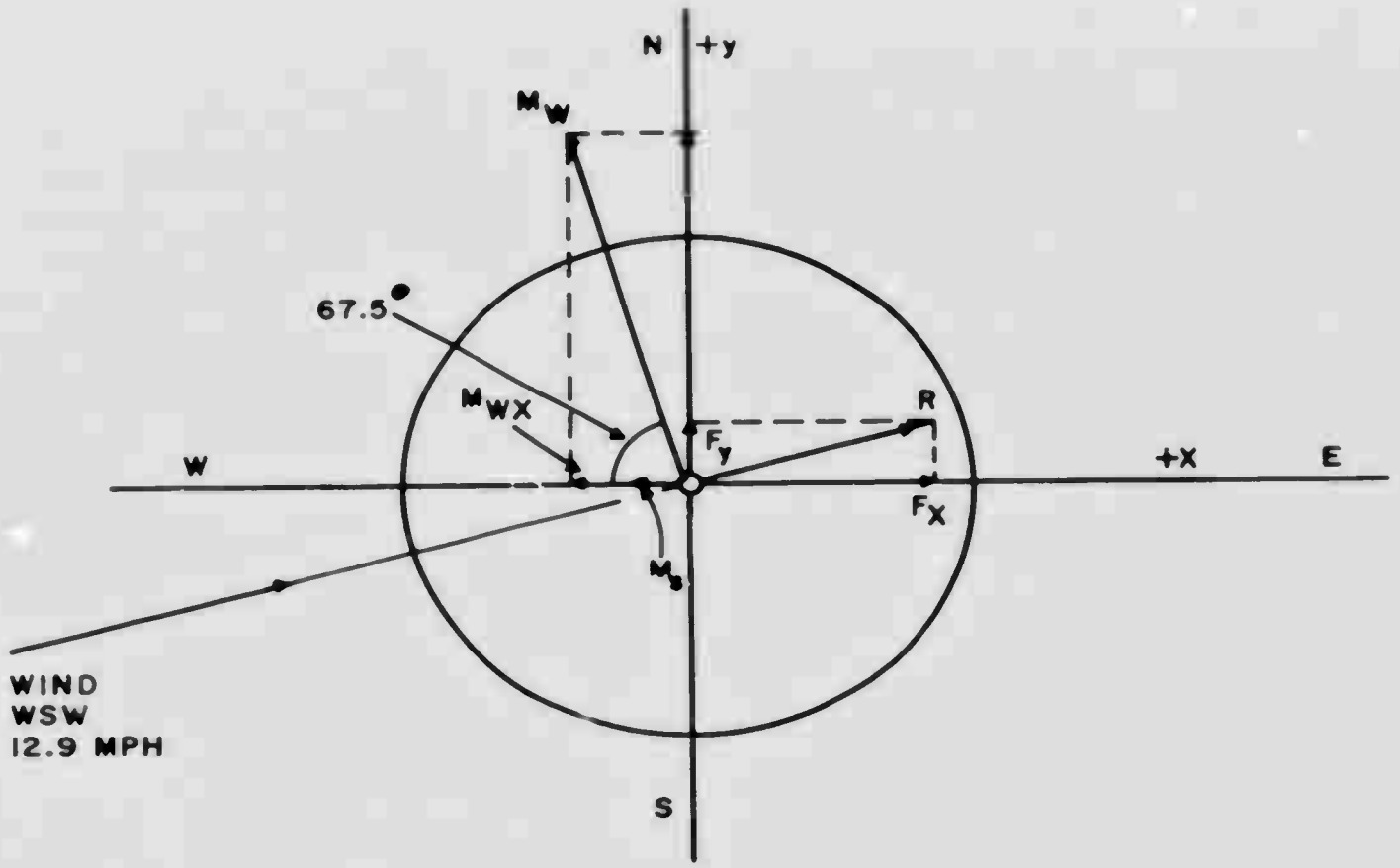

Figure 9. Resolution of External Bearing Loads, Case 1

Tables 5 and 6 should give identical wind direction. Only the estimated residual static overturning moment, which is compensated for in Table 6 can cause a disagreement.

Comparing the calculated directions (Table 5 and 6), the disagreement is pronounced. This indicates that the assumed residual overturning moment is inaccurate. Table 5 should yield the correct direction as the radial force is only due to the wind load. But the directions don't match the directly measured ones. If congruency in wind directions between Table 5 and Table 6 was present a backwards iteration could have been established to determine the correct residual static overturning moment.

Cases 3 and 4 were also analyzed using the measured four-point loads from Case 1 and 2. Results are similar to Cases 1 and 2. Cases 1a and 2a were also calculated using calculated four-point loads (no preload). Cases 1b and 2b are identical except that the four-point loads were calculated using a 0.002-inch preload. In all cases it was not possible to obtain consistent results between the imposed loads and the calculated resultants based on the measured ball loads.

The evaluation of static equilibrium for the antenna shows that the experimentally imposed test conditions, wind loads and added weight, are apparently masked by the inherent scatter in the test data. In addition, the assumed static unbalance of 126,400 in-lb appears to be inaccurate for the antenna on which the tests were made.

SECTION C. BEARING INTERNAL LOAD ANALYSIS

29. BEST Program. Reference 2 describes a computer program for calculating ball bearing internal load distribution and life for a given bearing geometry under specified loading conditions. For this study, the four-point contact ball bearing was viewed as two opposed, angular contact, single row bearings whose pitch circles were coincident. The program assumes rigid races.

Life calculations were made in accordance with the Lundberg-Palmgren statistical theory of rolling element bearing fatigue life. This method of life calculation was also used in the BDEP program described previously.

30. Static Load Tests. Case 1 through 4 of Table 7 are the computer input data for the four static load tests. Since complete load data was obtained for Cases 1 and 2, these cases were studied in detail. Figures 10 through 13 give a comparison between the measured ball loads and contact angle and the calculated values.

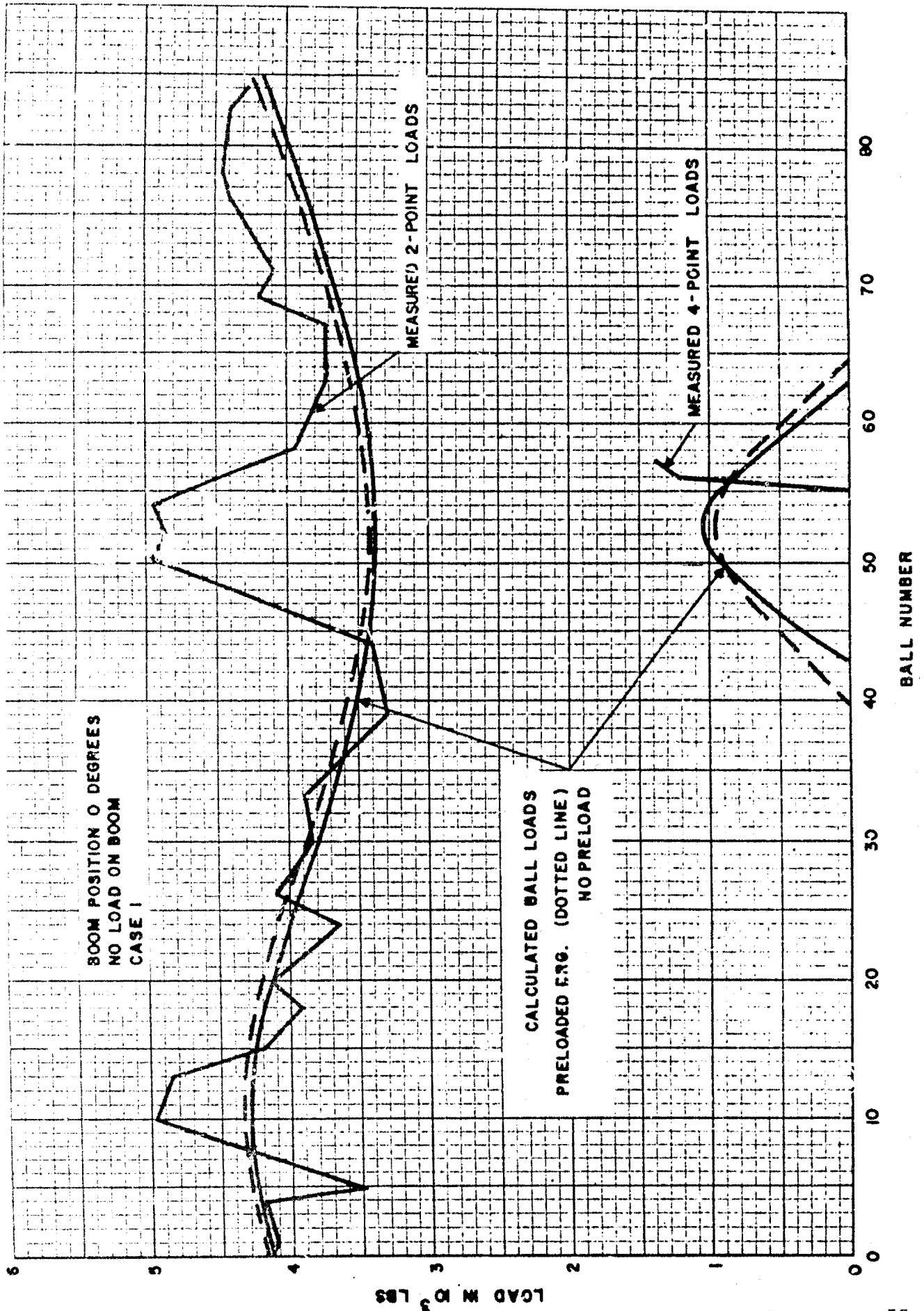

Figure 10. AN/FPS-24 Bearing Load Distribution, 0 Degrees, No Load on Boom

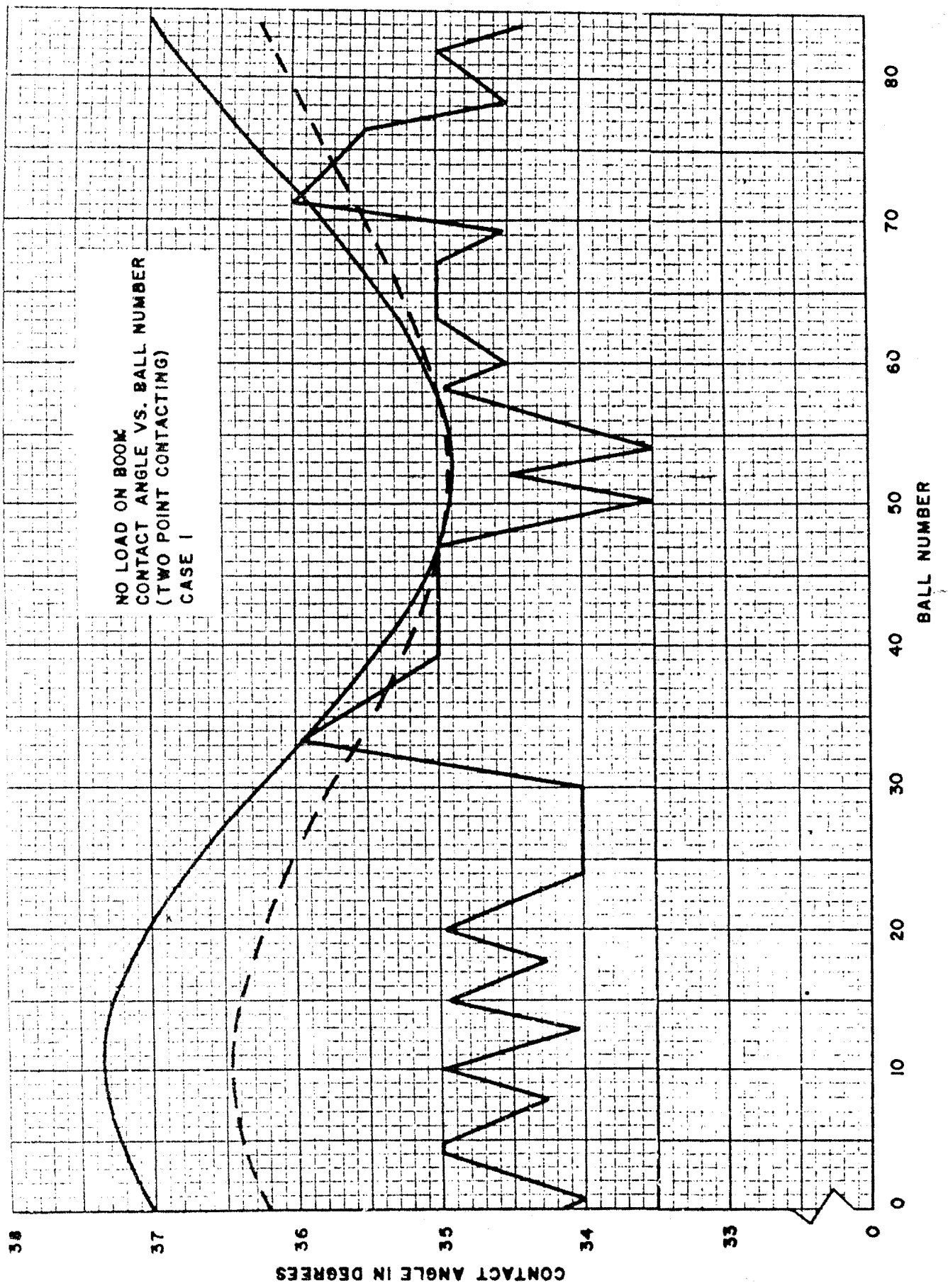

Figure 11. AN/FPS-24 Contact Angle Distribution, 0 Degrees, No Load on Boom

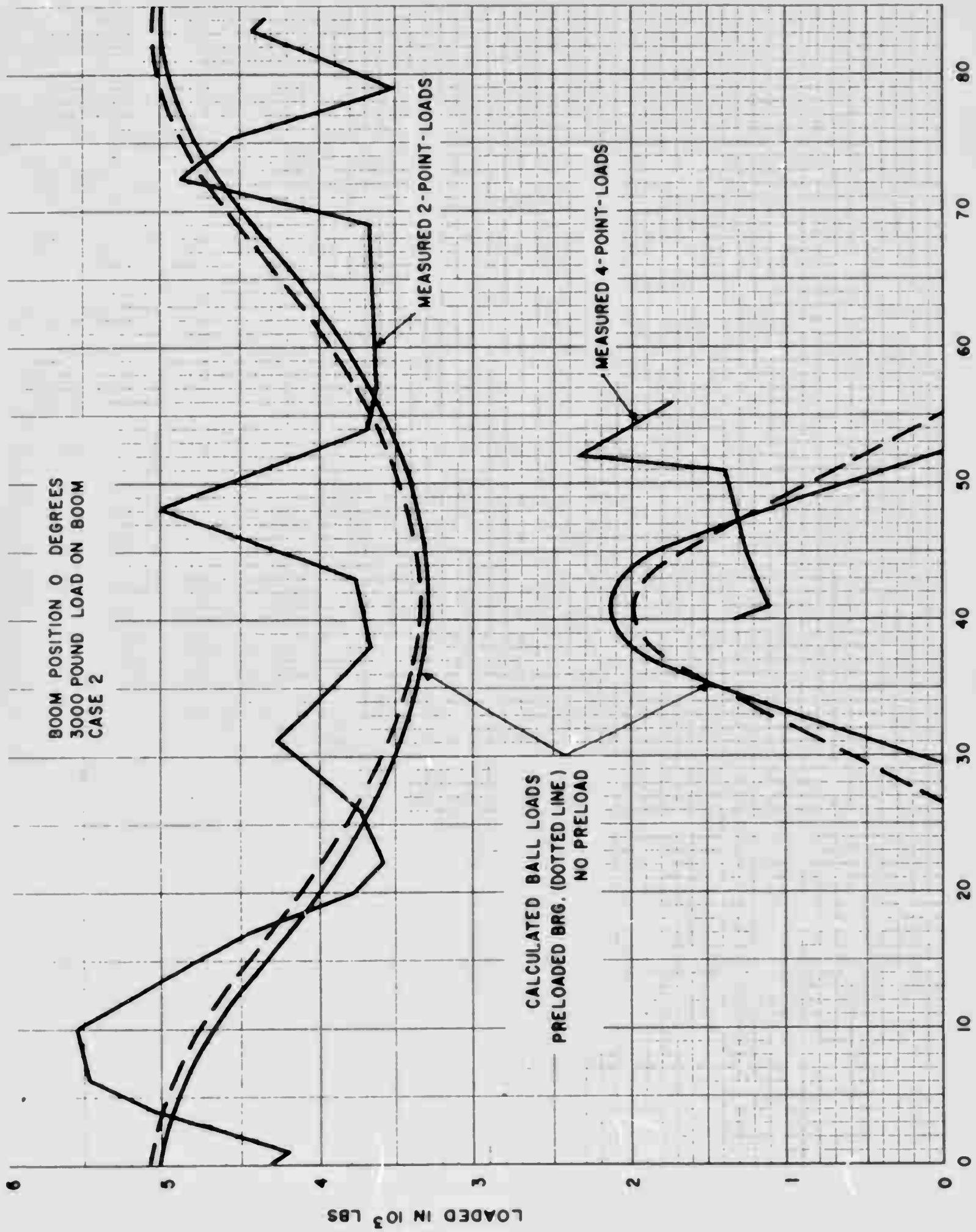

Figure 12. AN/FPS-24 Bearing Load Distribution, 0 Degrees, 3000 lbs. on Boom

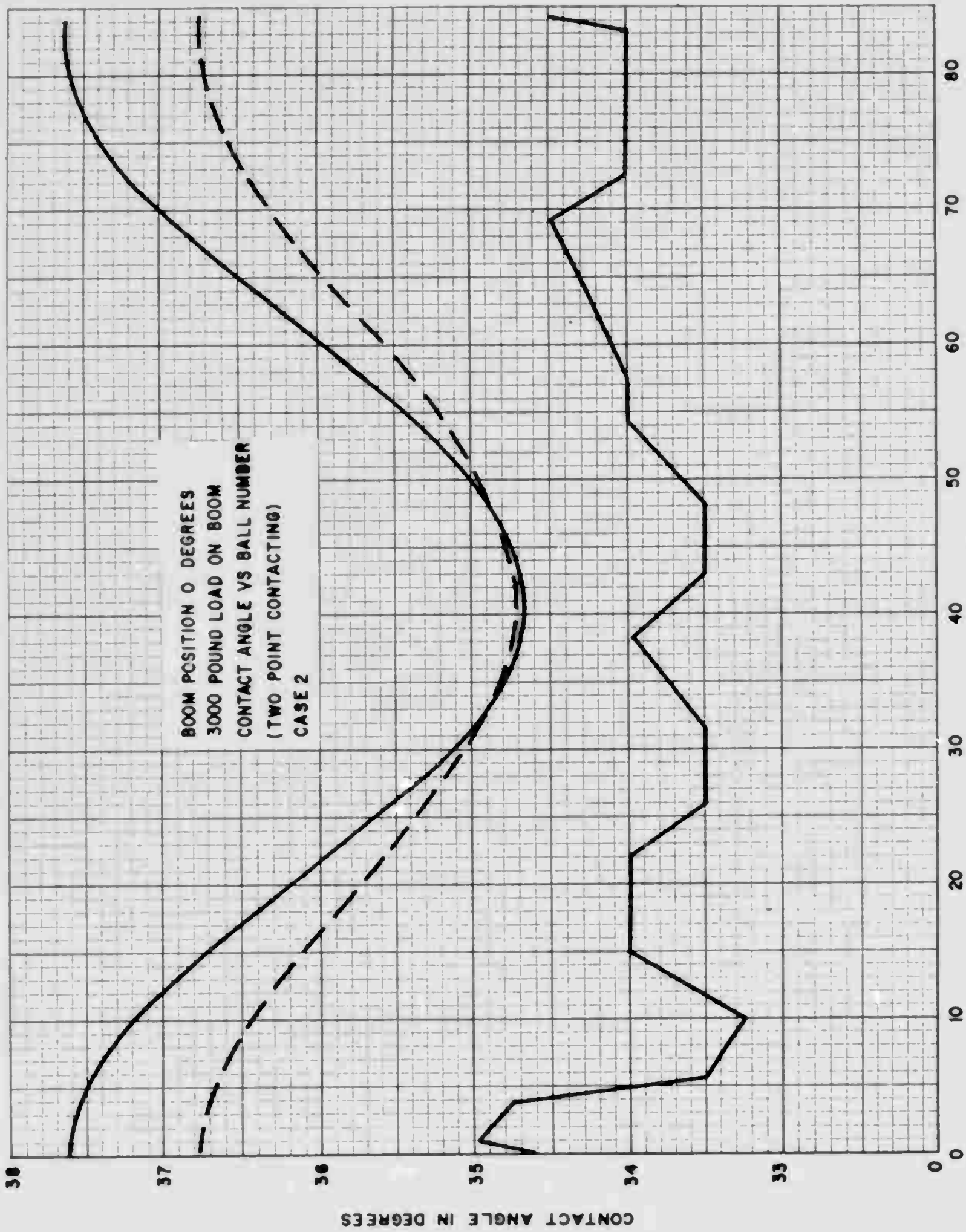

Figure 13. AN/FPS-24 Contact Angle Distribution, 0 Degrees, 3000 lbs. on Boom

The calculated curves show both the non-preloaded and preloaded cases corresponding to the 0 - 0.002 in. preload tolerance on the bearing. There is little difference between the two cases. The general level of the measured and calculated ball loads is close but the variation in their values is not. The two peaks in the measured data correspond to two of the corners of the boxlike structure on which the bearing is mounted. This indicates that the races are deforming and the support structure is stiffer at these two points than elsewhere.

The regions of calculated four-point contact correspond roughly to where the measured loads were picked up, and are of the same order of magnitude. On the average, the measured contact angles ran about two degrees less than the calculated values. This difference is also indicative of race deformation.

TABLE 7

BEST PROGRAM INPUT DATA

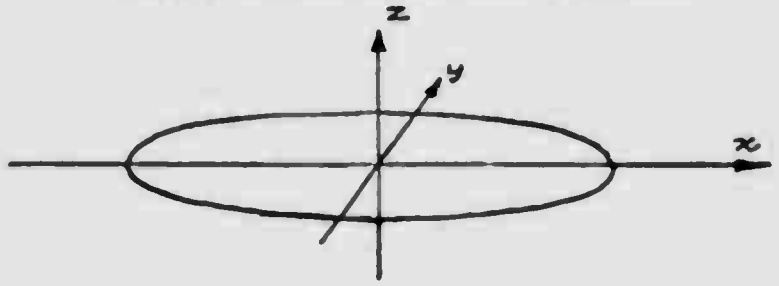

Case No.	Condition		Loads					
			Thrust lbs.	Radial lbs.		Moment in-lbs.		
	Boom Position	Load On Boom	F_z	F_x	F_y	M_x	M_y	M_z
1	0°	0	-181700	2770	1150	-586400	1110000	0
2	0°	3000	-184700	1554	1554	-2382400	600000	0
3	315°	0	-181700	2310	956	-509400	924000	0
4	315°	3000	-184700	1410	1410	-2348400	566000	0
5	-	0	-181700	0	-35500	8973600	0	0
6	-	0	-181700	0	-15800	4973600	0	0
7	-	0	-181700	0	-12000	3473600	0	0
8	-	0	-181700	0	-7000	2173600	0	0
9	-	0	-181700	0	-4000	1273600	0	0
10	A		-223700	0	-63000	20800000	0	0
11	B		-181700	0	-63000	20800000	0	0
12	C		-223700	0	-15700	5500000	0	0
13	D		-181700	0	-15700	5500000	0	0
14	E		-223700	0	-3930	1640000	0	0
15	F		-181700	0	-3930	1640000	0	0

31. Effect of Wind on Internal Load Distribution. Load Cases 5 through 9 were run to investigate the effect of higher wind velocities on the bearing internal load distribution. The ball load at $\theta = 138^{o}$ was measured for various wind velocities directed into the sail from the N (0^{o}). The ball loads measured as a function of wind velocity are shown in Table 8.

TABLE 8

MEASURED BALL LOAD VS WIND VELOCITY
$\theta = 138^{o}$

Wind Velocity (mph)	Load (lbs)
40	4200
30	4020
25	3970
20	3900
15	3820

Since the wind velocity and direction are known, the radial force and overturning moment can be read from Figure 7. Combining this with the static unbalance and weight determines the load on the bearing as shown in Table 9 below.

TABLE 9

DETERMINATION OF BEARING LOAD FOR VARIOUS WIND CONDITIONS

Case	Wind Velocity mph	Wind Loads		Net Moment	
		F_y lb	M_{wx} in-lb 10^6	M_x in-lb 10^6	F_z Weight lbs
5	40	-35500	9.1	8.9736	-181,700
6	30	-15800	5.1	4.9736	-181,700
7	25	-12000	3.6	3.4736	-181,700
8	20	-7000	2.3	2.1736	-181,700
9	15	-4000	1.4	1.2736	-181,700

Using the above bearing loads, the internal load was calculated using the BEST program. A comparison is made between the measured and calculated ball load at $\theta = 138^{o}$ in Figure 14. The calculated values exceed the measured, indicating that the assumed empirical drag coefficient is most likely higher than the actual value, or else the assumed antenna center of pressure is much lower than the 27-foot value cited in Figure 7. This conclusion is exactly opposite to the results of Section B where analysis of the ball loads indicated a higher wind loading than predicted using the emperical drag coefficient of Figure 7. Further analysis tends to indicate the emperical drag coefficient should be higher than the assumed value.

SECTION D. BEARING LIFE CALCULATIONS

32. Bearing Equivalent Load. The life calculations were made in accordance with the Lundberg-Palmgren theory of rolling-element bearing fatigue life. This theory is the basis for the AFBMA Standards No. 9 and 11 for calculating the fatigue lives of ball and roller bearings, respectively, and is also used by A. B. Jones in References 2 and 3.

The Lundberg-Palmgren theory gives the capacity of a ball race contact for 90 per cent probability of survival to 10^{6} revolutions as

$$Q_{cq} = A \left[\frac{2f}{2f - 1}\right]^{.41} \left[\frac{1 \pm \gamma \cos \beta_q}{1 \pm \gamma \cos \beta_q}\right]^{1/3} {}^{1.39\gamma} \; .3_d e_n - 1/3 \qquad (1)$$

where the upper sign is used for an inner race contact and the lower sign for an outer race contact.

For a raceway in which a particular point supports the same load at each ball passage, the life of the race in hours for 90 per cent probability of survival is

$$B^{L_1} = \frac{10^6}{60\ N\left[\frac{1}{n} \sum_{q=1}^{n} \left(\frac{P_q}{Q_{cq}}\right)^{10/3}\right] .9} \qquad (2)$$

For a raceway in which the loading of a particular point varies cyclically with time, the life of the raceway in hours for 90 per cent probability of survival is

$$B^{L_2} = \frac{10^6 n}{60\ N \sum_{q=1}^{n} \left(\frac{P_q}{Q_{cq}}\right)^{3}} \qquad (3)$$

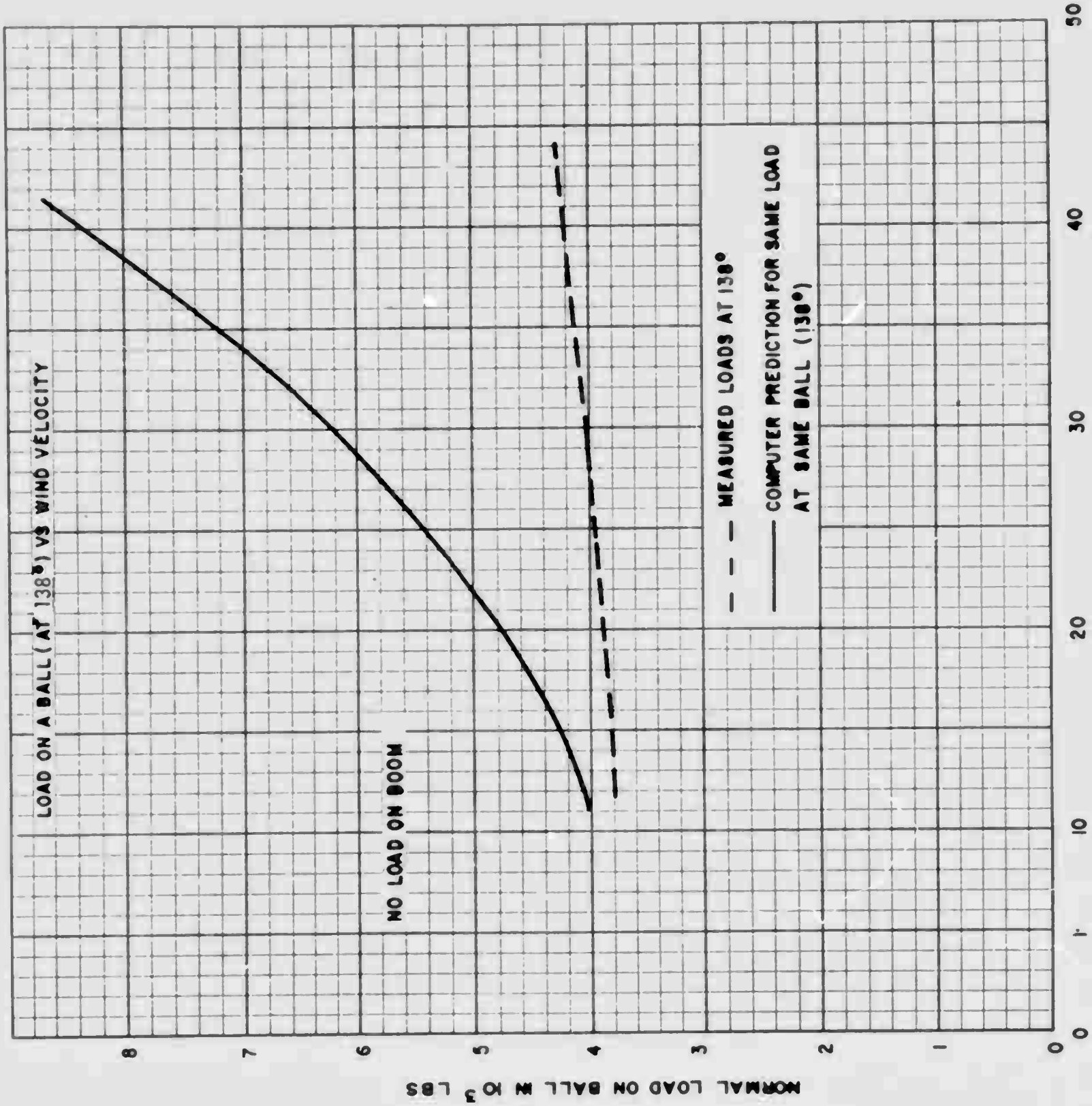

Figure 14. Calculated and Measured Ball Load Versus Wind Velocity

The life of the complete ball bearing is

$$B^L = \left[\left(\frac{1}{B^{L_1}} \right)^{10/9} + \left(\frac{1}{B^{L_2}} \right)^{10/9} \right]^{-.9} \qquad (4)$$

Similar equations for roller bearings in which line contact exists are given in Reference 2.

The value of the exponent e for small size bearings is taken as 1.8. For balls larger than one inch in diameter, generally poorer life is obtained, and to account for this the constant e is reduced to 1.4.

The dynamic capacity for each race can be computed from equation (1), and is

$$Q_{ci} = 10,158 \text{ lbs}$$

$$Q_{co} = 11,038 \text{ lbs}$$

In comparing the effect of different bearing load distributions on bearing life it sometimes is convenient to determine an equivalent ball load defined as

$$P_{er} = \left[\frac{1}{n} \sum_{\phi = 1}^{n} P_\phi^3 \right]^{1/3}$$

For the race which rotates with respect to load (outer race) (5)

$$P_{es} = \left[\frac{1}{n} \sum_{\phi = 1}^{n} P_\phi^{10/3} \right]^{3/10}$$

For the race which is stationary with respect to load (inner race) (6)

Equivalent ball loads can be calculated for the measured load distributions of Cases 1 and 2 for which complete data is available. These are presented in Table 10.

TABLE 10

EQUIVALENT BALL LOADS FOR MEASURED LOAD DISTRIBUTION

Case	Major Axis Loads		Minor Axis Loads		Total Bearing Life hrs.
	P_{es} lbs	P_{er} lbs	P_{es} lbs	P_{er} lbs	
1	4160	4160	435	383	29,370
2	4300	4260	1010	940	26,690

Equivalent ball loads can also be computed for the computer determined load distribution. This is presented in Table 11 below.

TABLE 11

EQUIVALENT BALL LOADS FOR COMPUTED LOAD DISTRIBUTION

Case	Major Axis Loads P_{es}	Major Axis Loads P_{er}	Minor Axis Loads P_{es}	Minor Axis Loads P_{er}	Total Bearing Life (.002 inch preload) Hours
1	3906	3910	508	482	35, 100
2	4248	4254	1072	476	27, 200

A comparison of Tables 10 and 11, shows close agreement for Case 2 between the bearing life based on the measured static load distribution and that based on the computed static load distribution.

The discrepancy for Case 1 is larger but it is within the accuracy of the data. Reference to Table 4 shows that the static equilibrium check indicates that the measured ball loads for Case 1 are about 7 per cent higher than they should be to support the weight of the antenna. From equations (5) and (6), P_{es} and P_{er} will be roughly 7 per cent high. Since the life is inversely proportional to the load cubed, this would cause about a 22 per cent reduction in life calculated from 35, 100 to 28, 700 hours. Thus the inherent inaccuracy in the load data could account for the discrepancy between the bearing life computed from the measured load data and that determined from the computed load distribution. In this connection, it should be noted that for Case 2, in which agreement between the two lifes based on measured and computed load distributions is good, the static equilibrium check is also close, 184, 700 pounds versus 182, 040 pounds.

Although the shape of the measured and computed load distributions differ, somewhat, there is no significant difference between the measured equivalent bearing load and computed equivalent bearing load.

33. Design Bearing Life. The load schedule used by Jones in Reference 3 does not agree exactly with that in Table 2. For this reason, the bearing life was recalculated using the bearing load schedule of Table 2.

In order to check the BEST program against the results of Reference 3, a sample load case for the 13-knot (no ice) condition from Table 8 of Reference 3 was run. The BEST program produced a life of 26, 278 hours ersus a predicted life of 25, 573 hours from Reference 3 for the same load conditions. It is felt the agreement is close enough to insure compatibility between the two calculation methods.

Table 12 gives the bearing lifes for continuous operation at the loads given in Table 2.

TABLE 12

DESIGN BEARING LIFE

Wind Velocity Knots	No Preload			0.002 Inch Preload		
	Major Axis	Minor Axis	Total	Major Axis	Minor Axis	Total
52 (ice)	1782	4680	1368	1701	5840	1330
52 (no ice)	2080	4630	1525	1990	4800	1490
26 (ice)	11, 862	215, 716	11, 452	11, 200	230, 500	10, 800
26 (no ice)	18, 013	207, 789	17, 006	16, 940	227, 500	16, 100
13 (ice)	19, 995	8, 209, 000	19, 972	19, 020	8, 140, 000	19, 000
13 (no ice)	35, 020	7, 138, 700	34, 935	33, 150	7, 690, 000	33, 100
Prorated life	21, 050				20, 450	

34. Extension of Results to the X-Type Roller. Because the geometry of the X-type roller bearing is different from the four-point contact type, it is not possible to directly transfer a measured load distribution from one bearing type to another. The conclusion of this study is that the equivalent ball loads and consequently the bearing lifes for the calculated and measured load distributions do not differ significantly. Assuming that this result can be extrapolated to the X-type roller, the rigid race analysis used by Jones in Reference 3, should give the same life as a calculation based on a measured load distribution.

Table 13 is the calculated bearing life for the X-type roller (Messinger 22590) for the load schedule of Table 2.

TABLE 13

BEARING DESIGN LIFE X-TYPE ROLLER
MESSINGER 22590

Load Case	Bearing Life Hours
A	1, 820
B	2, 021
C	53, 084
D	86, 746
E	139, 160
F	299, 200
Prorated Life	90, 660

As in the case for the four-point contact bearing, these results differ from those of Table 13 of Reference 3, because a higher wind moment loading is used in the load schedule of Reference 3 than was used in this study.

SECTION E. CONCLUSIONS

The evaluation of static equilibrium for the test antenna shows that the experimentally imposed loads, low velocity wind loads, and added boom weight, are masked by the inherent scatter in the test data. The capability to produce larger moment loads, thus better simulating higher velocity wind loads, would result in a condition which is much more amenable to discrimination of differences in ball loads due to other than pure thrust loading.

Within the accuracy of the test data, it was found that for the four-point contact bearing there was no significant difference between the equivalent ball load based on the measured load distribution and that based on the computed load distribution for the same bearing load conditions.

Extension of the data to the x-type roller bearing results in no significant difference in previously calculated life estimates.

Design bearing life shown in Table 12 is based on the calculated loads given in Table 2. Since there was no significant difference between the measured load distribution and the computed load distribution, the design bearing life would be the same, and no separate table is shown based on measured load distribution.

REFERENCES

1. Precision Runout Measurements, Main Bearing and Seats, AN/FPS-24 Antenna, Cottonwood, Idaho.

2. Jones, A. B., "A General Theory for Elastically Constrained Ball and Radial Roller Bearing Under Arbitrary Load and Speed Conditions," Bearing Systems Program (BFST), Fafnir Bearing Company, New Britain, Connecticut.

3. Jones, A. B., "A Theoretical Investigation of Large Rolling Element Bearing Performance in FPS-24 and FPS-35 Radar Antenna Service," Rome Air Development Center, Contract No. AF30(602)-3326.

4. New Departure - Analysis of Stresses and Deflections Vols. I - II, New Departure Div., General Motors Corporation 1946.

APPENDIX I

CALCULATED CONTACT ELLIPSE

Two methods of load measurement were used in determining the individual ball loads, the load cell method and the contact ellipse method both of which are described in the experimental part of this report. When the ball is pressed against the race, local elastic deformation occurs at the point of contact. The dimensions of the contact area are a measure of the imposed load. In order to gain some indication of the accuracy of this method, a sample ball and race were placed in a hydraulic press and the contact ellipse major and minor axes were measured for various loads. Using the equations of Reference 4, the dimensions of the contact ellipse for a ball and race of the AN/FPS-24 antenna bearing were calculated as a function of load.

Figures I-1 and I-2 give a comparison between the calculated and measured values. The agreement is very good, and provides a check on the accuracy of the contact ellipse method.

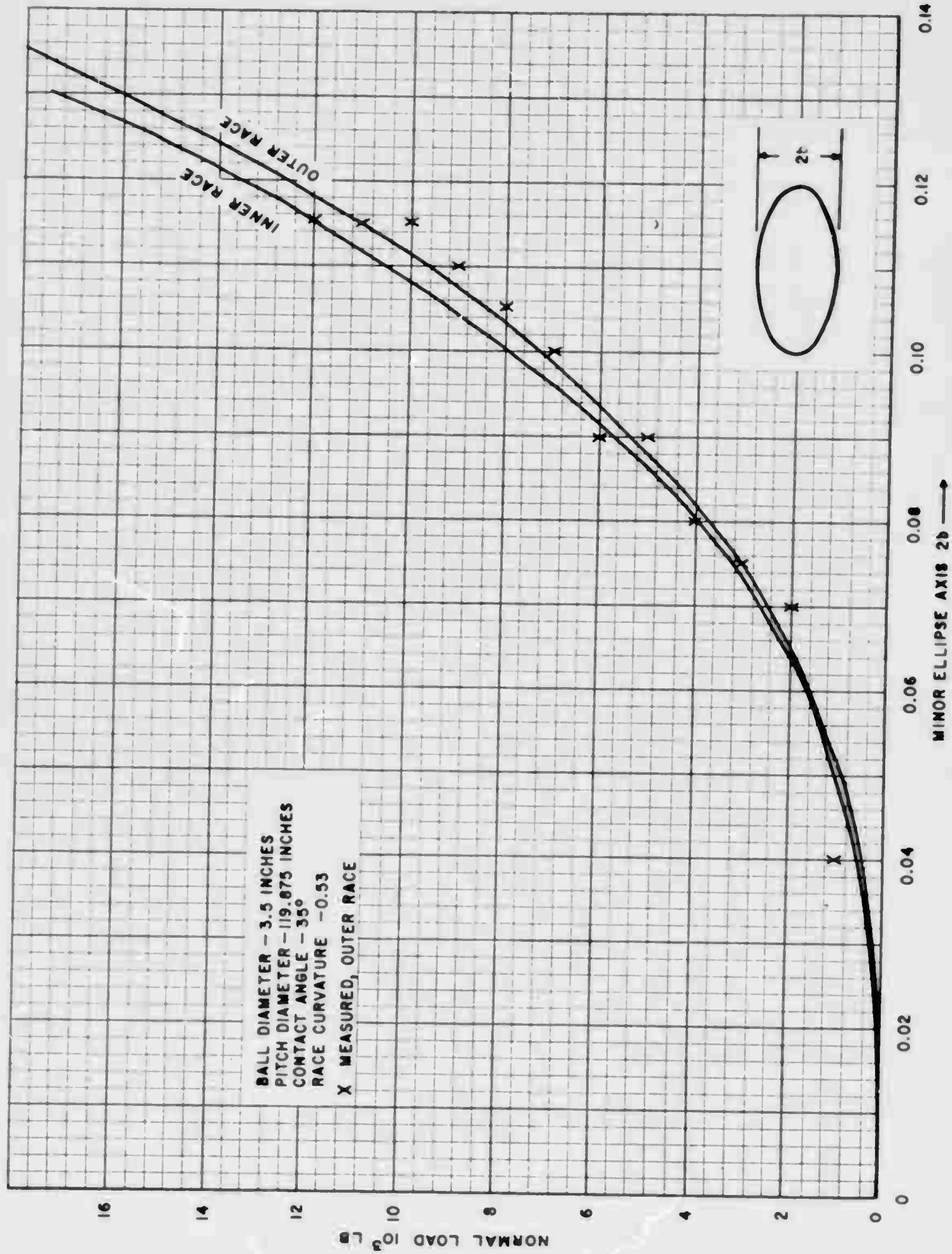

Figure A-1. Ball Load Versus Ellipse Minor Axis

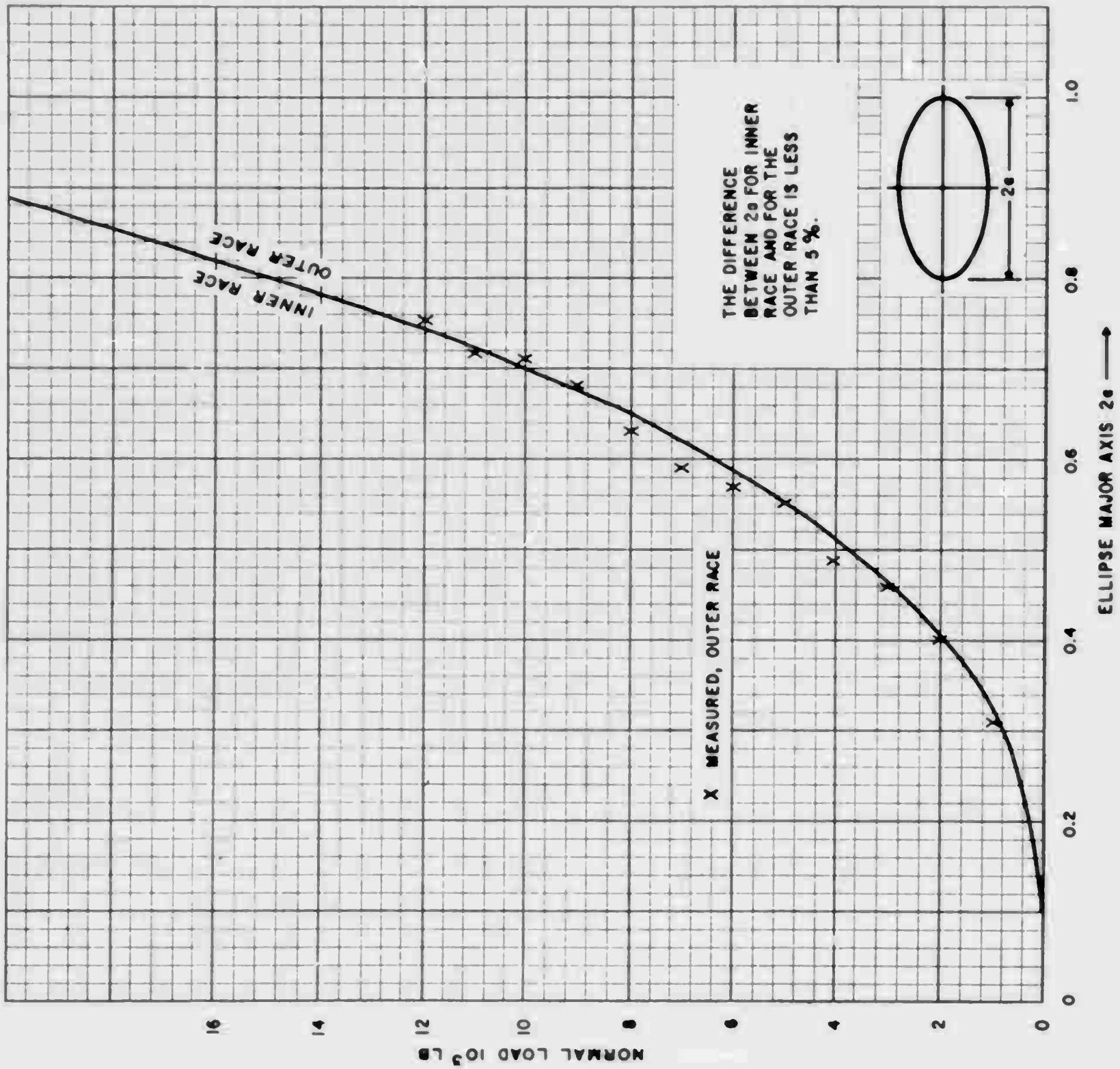

Figure A-2. Ball Load Versus Ellipse Major Axis

TABLE A-1

ACCURACY OF METHODS OF MEASUREMENT

	Method	Accuracy	Repeatability
1.	Contact Angle	± 1 1/2°	± 1/2°
2.	Static Load Cell (from pounds to readout	± 5%	± 1 1/2%
3.	Load Ellipse	± 7%	± 7%
4.	Dynamic Ball Caliper	± 10%	± 5%

Note: Accuracy for method number 4 pertains to data that could be obtained from a refined calipered ball device and not to the dynamic feasibility data presented in this report.

Unclassified
Security Classification

DOCUMENT CONTROL DATA - R&D

(Security classification of title, body of abstract and indexing annotation must be entered when the overall report is classified)

1 ORIGINATING ACTIVITY (Corporate author)
General Electric Co.
Heavy Military Electronics Dept.
Syracuse, N.Y.

2a REPORT SECURITY CLASSIFICATION
Unclassified

2b GROUP

3 REPORT TITLE
Structural Study of AN/FPS-24 Pedestal

4 DESCRIPTIVE NOTES (Type of report and inclusive dates)
Final Report

5 AUTHOR(S) (Last name, first name, initial)
Barnhart, H. D.
McCrew, J. M.
Lange, E.

6 REPORT DATE
September 1965

7a TOTAL NO. OF PAGES
88

7b NO. OF REFS
4

8a CONTRACT OR GRANT NO.
AF30(602)-3567

b PROJECT NO.

c System 416L

d

9a ORIGINATOR'S REPORT NUMBER(S)
EH-61655

9b OTHER REPORT NO(S) (Any other numbers that may be assigned this report)
RADC-TR-65-247

10 AVAILABILITY/LIMITATION NOTICES
Available at DDC and CFSTI.

11 SUPPLEMENTARY NOTES

12 SPONSORING MILITARY ACTIVITY
Rome Air Development Center
Griffiss Air Force Base, New York

13 ABSTRACT
Results are presented from an investigation of the load distribution to the main azimuth bearing of the AN/FPS-24 radar. The bearing is a 10-ft diameter 4-point contact bearing subjected to thrust, radial, and overturning loads. Actual static ball loads were determined in a field test. Bearing life calculations based on the measured loads and compared with theoretical calculations are presented. The feasibility of making dynamic measurements of ball loads under actual rotation condition was proven.

DD FORM 1 JAN 64 1473

Unclassified
Security Classification

Unclassified

Security Classification

14 KEY WORDS	LINK A		LINK B		LINK C	
	ROLE	WT	ROLE	WT	ROLE	WT
Large diameter rolling element bearings Anti-friction bearings FPS-24 Pedestal study Rolling bearing load distribution Radar equipment						

INSTRUCTIONS

1. ORIGINATING ACTIVITY: Enter the name and address of the contractor, subcontractor, grantee, Department of Defense activity or other organization *(corporate author)* issuing the report.

2a. REPORT SECURITY CLASSIFICATION: Enter the overall security classification of the report. Indicate whether "Restricted Data" is included. Marking is to be in accordance with appropriate security regulations.

2b. GROUP: Automatic downgrading is specified in DoD Directive 5200.10 and Armed Forces Industrial Manual. Enter the group number. Also, when applicable, show that optional markings have been used for Group 3 and Group 4 as authorized.

3. REPORT TITLE: Enter the complete report title in all capital letters. Titles in all cases should be unclassified. If a meaningful title cannot be selected without classification, show title classification in all capitals in parenthesis immediately following the title.

4. DESCRIPTIVE NOTES: If appropriate, enter the type of report, e.g., interim, progress, summary, annual, or final. Give the inclusive dates when a specific reporting period is covered.

5. AUTHOR(S): Enter the name(s) of author(s) as shown on or in the report. Enter last name, first name, middle initial. If military, show rank and branch of service. The name of the principal author is an absolute minimum requirement.

6. REPORT DATE: Enter the date of the report as day, month, year; or month, year. If more than one date appears on the report, use date of publication.

7a. TOTAL NUMBER OF PAGES: The total page count should follow normal pagination procedures, i.e., enter the number of pages containing information.

7b. NUMBER OF REFERENCES: Enter the total number of references cited in the report.

8a. CONTRACT OR GRANT NUMBER: If appropriate, enter the applicable number of the contract or grant under which the report was written.

8b, 8c, & 8d. PROJECT NUMBER: Enter the appropriate military department identification, such as project number, subproject number, system numbers, task number, etc.

9a. ORIGINATOR'S REPORT NUMBER(S): Enter the official report number by which the document will be identified and controlled by the originating activity. This number must be unique to this report.

9b. OTHER REPORT NUMBER(S): If the report has been assigned any other report numbers *(either by the originator or by the sponsor)*, also enter this number(s).

10. AVAILABILITY/LIMITATION NOTICES: Enter any limitations on further dissemination of the report, other than those imposed by security classification, using standard statements such as:

(1) "Qualified requesters may obtain copies of this report from DDC."

(2) "Foreign announcement and dissemination of this report by DDC is not authorized."

(3) "U. S. Government agencies may obtain copies of this report directly from DDC. Other qualified DDC users shall request through

_____."

(4) "U. S. military agencies may obtain copies of this report directly from DDC. Other qualified users shall request through

_____."

(5) "All distribution of this report is controlled. Qualified DDC users shall request through

_____."

If the report has been furnished to the Office of Technical Services, Department of Commerce, for sale to the public, indicate this fact and enter the price, if known.

11. SUPPLEMENTARY NOTES: Use for additional explanatory notes.

12. SPONSORING MILITARY ACTIVITY: Enter the name of the departmental project office or laboratory sponsoring *(paying for)* the research and development. Include address.

13. ABSTRACT: Enter an abstract giving a brief and factual summary of the document indicative of the report, even though it may also appear elsewhere in the body of the technical report. If additional space is required, a continuation sheet shall be attached.

It is highly desirable that the abstract of classified reports be unclassified. Each paragraph of the abstract shall end with an indication of the military security classification of the information in the paragraph, represented as *(TS)*, *(S)*, *(C)*, or *(U)*.

There is no limitation on the length of the abstract. However, the suggested length is from 150 to 225 words.

14. KEY WORDS: Key words are technically meaningful terms or short phrases that characterize a report and may be used as index entries for cataloging the report. Key words must be selected so that no security classification is required. Identifiers, such as equipment model designation, trade name, military project code name, geographic location, may be used as key words but will be followed by an indication of technical context. The assignment of links, rules, and weights is optional.

Unclassified

Security Classification